

Supporting Information

Fully-fused boron-doped olympicenes: modular synthesis, tunable optoelectronic properties, and one-electron reduction

Jing Guo,^{‡a} Kaihua Zhang,^{‡a} Yanpei Wang,^a Haipeng Wei,^a Wang Xiao,^a Kun Yang,^{*a} Zebing Zeng^{*a}

^aState Key Laboratory of Chemo/Biosensing and Chemometrics, College of Chemistry and Chemical Engineering, Hunan University, Changsha 410082 (P. R. China), and Shenzhen Research Institute of Hunan University, Shenzhen 518000 (P. R. China)

Table of Contents

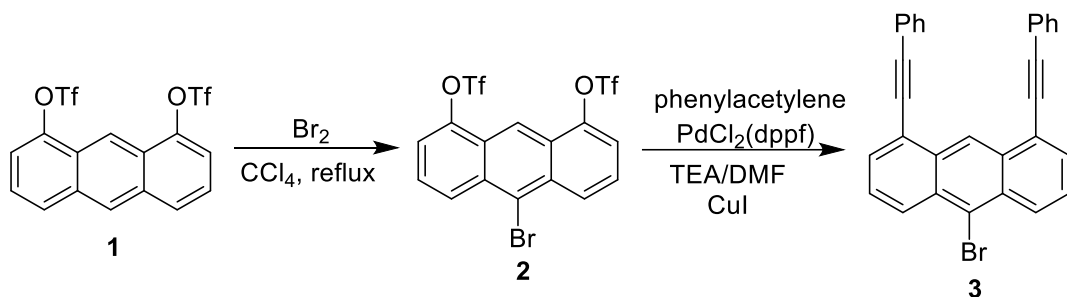
1. General method	S3
2. Synthetic procedures	S3
3. Single-crystal X-Ray analysis	S10
4 TD-DFT simulations of 11a-boraolympicenes.....	S11
5. Additional photophysical properties of 11a-boraolympicenes	S17
6 TD-DFT simulations of (BO-2) ⁻	S18
7 FT-IR spectra of BO-2 and (BO-2) ⁻	S20
8. NMR and mass spectra of all new compounds.....	S21
9. References	S49

1. General method

The commercially available compounds and solvents were used without further purification. Other solvents for special use were purified and dried by standard methods prior to use. Column chromatography was generally performed on silica gel (200 - 300 mesh) and reactions were monitored by thin layer chromatography (TLC) using silica gel GF254 plates with UV light to visualize the course of reaction. NMR data were recorded on a 400 MHz spectrometer using CDCl_3 or CD_2Cl_2 as solvent at room temperature. The chemical shifts (δ) are reported in ppm and coupling constants (J) in Hz. ^1H NMR chemical shifts were referenced to CDCl_3 (7.26 ppm). ^{13}C NMR chemical shifts were referenced to CDCl_3 (77.00 ppm). ^{11}B NMR chemical shifts were referenced to the external standard boron signal of $\text{BF}_3\cdot\text{Et}_2\text{O}$ (0 ppm). The following abbreviations were used to explain the multiplicities: *s* = singlet, *d* = doublet, *t* = triplet, *m* = multiplet. MALDI-TOF mass spectra (MS) were recorded on a Bruker Autoflex instrument using anthracene-1,8,9-triol as matrix. Cyclic voltammetry (CV) and differential pulse voltammetry (DPV) were performed on a Chenhua 650D electrochemical using a three-electrode cell with a glassy carbon working electrode, a platinum wire counter electrode, and an Ag/AgCl reference electrode in anhydrous solvents containing tetra-*n*-butyl-ammoniumhexafluorophosphate (TBAPF₆, 0.1 M) as supporting electrolyte at 298 K. All the potentials were externally calibrated by a ferrocene/ferrocenium couple. Steady-state UV-vis absorption spectra were recorded on a Shimadzu UV-3600 spectrometer. ESR spectra were recorded on a JES-FA200 spectrometer. Photoluminescence spectra were recorded on a Thermo Scientific Lumina. HR MALDI-TOF mass spectra were recorded on Finnigan MAT TSQ 7000 instrument. IR spectra were recorded on SHIMADZU IRSpirit-T and reported in unit of cm^{-1} .

2. Synthetic procedures

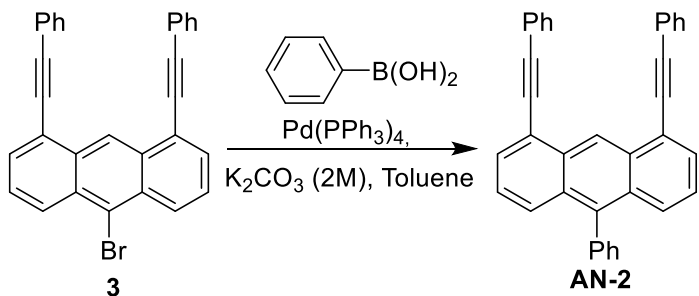
10-bromo-1,8-bis(phenylethynyl)anthracene (3)



To a solution of compound **1** (5 g, 10.5 mmol, 1.0 equiv.) in CCl_4 (300 mL), Br_2 (2.7 mL, 52.5 mmol, 5.0 equiv.) was added slowly at room temperature. The mixture was heated to reflux and

monitored by TLC to confirm consumption of starting material. Upon completion, the mixture was cooled down to room temperature and then quenched with 1 M sodium thiosulfate. The organic layer was collected, and the remaining aqueous solution was further extracted by ethyl acetate. After removing the organic solvents under reduced pressure, the residue was purified by silica gel chromatography (eluent: petroleum ether/ethyl acetate = 20:1) to give compound **2** as a faint yellow solid in 81% yield (4.7 g). ¹H NMR (400 MHz, CDCl₃): δ 8.93 (s, 1H), 8.58 (d, J = 8.6 Hz, 2H), 7.66 (m, 4H); ¹³C NMR (100 MHz, CDCl₃): δ 146.57, 132.98, 128.48, 127.20, 125.76, 124.33, 122.46, 120.30, 118.41, 117.12, 114.20. To a solution of compound **2** (5.5 g, 10 mmol, 1.0 equiv.) in DMF/TEA (1:1) mixed solution, CuI (190 mg, 1 mmol, 0.1 equiv) was added. After stirring about 0.5 h at room temperature, phenylacetylene (2.1 g, 21 mmol, 2.1 equiv) and PdCl₂(dpff) (370 mg, 0.5 mmol, 0.05 equiv) were added and monitored by TLC to confirm consumption of starting material. Upon completion, the mixture was quenched with 200 mL water. The organic layer was collected, and the remaining aqueous solution was further extracted by ethyl acetate. After removing the organic solvents under reduced pressure, the residue was purified by silica gel chromatography (eluent: petroleum ether/CH₂Cl₂ = 20:1) to give compound **3** as a yellow solid in 85% yield (3.9 g). ¹H NMR (400 MHz, CDCl₃): δ 9.71 (s, 1H), 8.54 (d, J = 8.9 Hz, 2H), 7.84 (d, J = 6.9 Hz, 2H), 7.63 – 7.59 (m, 2H), 7.57 (d, J = 7.7 Hz, 4H), 7.34 (t, J = 7.4 Hz, 2H), 7.20 (t, J = 7.6 Hz, 4H); ¹³C NMR (100 MHz, CDCl₃): 132.22, 131.69, 130.78, 130.37, 128.38, 126.80, 124.67, 123.62, 123.03, 121.97, 121.15, 120.80, 94.30, 88.29. MS (MALDI-TOF, m/z): calcd for C₃₀H₁₇Br [M]⁺, 456.0514, found 456.0513, (error = -2.2 ppm).

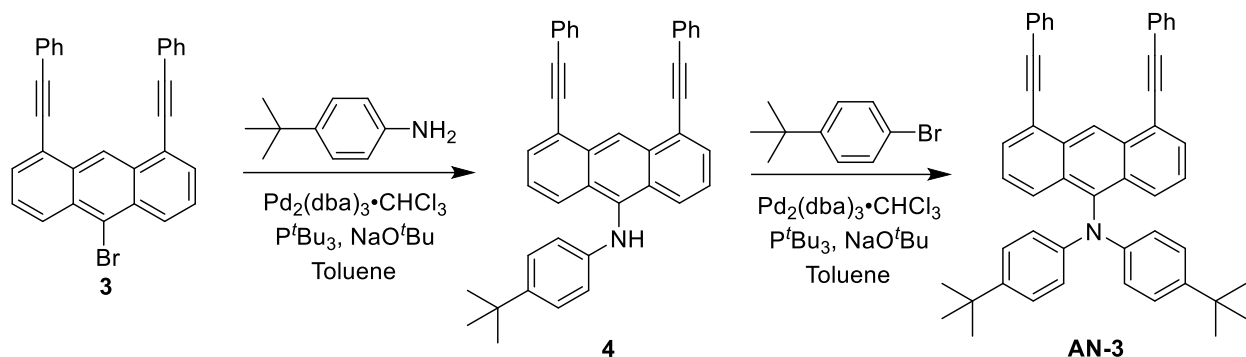
10-phenyl-1,8-bis(phenylethyynyl)anthracene (AN-2)



To a solution of compound **3** (300 mg, 0.66 mol, 1.0 equiv.) in toluene/EtOH/H₂O (9:5:1), phenylboronic acid (96 mg, 0.79 mmol, 1.2 equiv.), aqueous solution of K₂CO₃ (2 M, 2 mL) and Pd(PPh₃)₄ (38 mg, 0.033 mmol, 0.05 equiv.) were added under an argon atmosphere. The mixture was stirred at 95 °C and monitored by TLC to confirm consumption of starting material. Upon completion, the resulting solution was washed with water, extracted with ethyl acetate and

dried over anhydrous Na_2SO_4 . After filtration and removal of the solvents, the crude product was purified by silica gel chromatography (eluent: petroleum ether/ CH_2Cl_2 = 20:1) to give compound **AN-2** as a yellow solid in 91% yield (272 mg). ^1H NMR (400 MHz, CD_2Cl_2): δ 9.77 (s, 1H), 7.84 (d, J = 6.9 Hz, 2H), 7.69 (d, J = 10.1 Hz, 2H), 7.66 – 7.61 (m, 6H), 7.60 (m, 1H), 7.45 (m, 2H), 7.41 – 7.36 (m, 4H), 7.27 (t, J = 7.6 Hz, 4H); ^{13}C NMR (100 MHz, CD_2Cl_2): δ 138.92, 138.71, 132.17, 131.62, 131.44, 130.95, 130.56, 128.91, 128.86, 128.83, 128.24, 128.15, 125.51, 124.28, 123.60, 121.79, 95.31, 87.34. MS (MALDI-TOF, m/z): calcd for $\text{C}_{36}\text{H}_{22}$ [M] $^+$, 454.1722, found 454.1720, (error = -0.4 ppm).

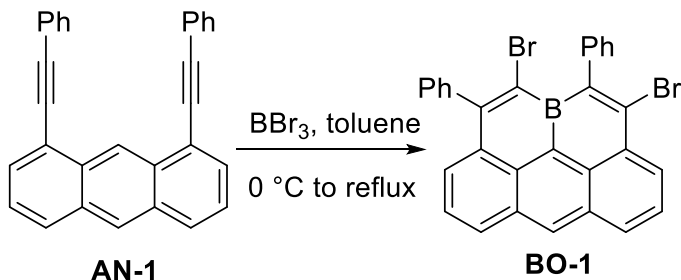
N,N-bis(4-(*tert*-butyl)phenyl)-4,5-bis(phenylethyynyl)anthracen-9-amine (AN-3)



To a solution of the compound **3** (500 mg, 1.09 mmol, 1 equiv) in dry toluene, 4-*tert*-Butylaniline (180 mg, 1.20 mmol, 1.1 equiv), sodium *tert*-butoxide (133 mg, 1.36 mmol, 1.25 equiv), $\text{Pd}_2(\text{dba})_3\cdot\text{CHCl}_3$ (113 mg, 0.11 mmol, 0.1 equiv) and P^tBu_3 (0.26 ml of a 10% solution in hexane, 0.11 mmol, 0.1 equiv) were added under an argon atmosphere. The mixture was heated to 80 °C and monitored by TLC to confirm consumption of starting material. Upon completion, the resulting solution was washed with water, extracted with ethyl acetate and dried over anhydrous Na_2SO_4 . After filtration and removal of the solvents, the crude product was purified by silica gel chromatography (eluent: petroleum ether/ CH_2Cl_2 = 10:1) to give compound **4** as a yellow solid in 87% yield (501 mg). ^1H NMR (400 MHz, CDCl_3): δ 9.57 (s, 1H), 8.19 (d, J = 8.8 Hz, 2H), 7.79 (d, J = 6.7 Hz, 2H), 7.60 (d, J = 7.4 Hz, 4H), 7.43 – 7.39 (t, J = 7.8 Hz, 2H), 7.35 (t, J = 7.4 Hz, 2H), 7.23 (m, 4H), 7.15 (d, J = 8.4 Hz, 2H), 6.50 (d, J = 8.4 Hz, 2H), 5.95 (s, 1H), 1.27 (s, 9H); ^{13}C NMR (100 MHz, CDCl_3): δ 144.51, 140.66, 135.19, 132.17, 130.66, 128.93, 128.41, 126.07, 125.44, 124.77, 123.25, 122.46, 121.88, 96.4986, 87.73, 36.53, 32.14. MS (MALDI-TOF, m/z): calcd for $\text{C}_{40}\text{H}_{31}\text{N}$ [M] $^+$, 525.2457, found 525.2454, (error = -0.6 ppm). To a solution of compound **AN-3** (300 mg, 0.57 mmol, 1 equiv) in dry toluene, 4-*tert*-Butylaniline (135 mg, 0.63 mmol, 1.1 equiv), sodium *tert*-butoxide (68 mg, 0.71 mmol, 1.25 equiv), $\text{Pd}_2(\text{dba})_3\cdot\text{CHCl}_3$ (62 mg, 0.06 mmol, 0.1 equiv) and P^tBu_3 (0.14 mL of a 10% solution in hexane,

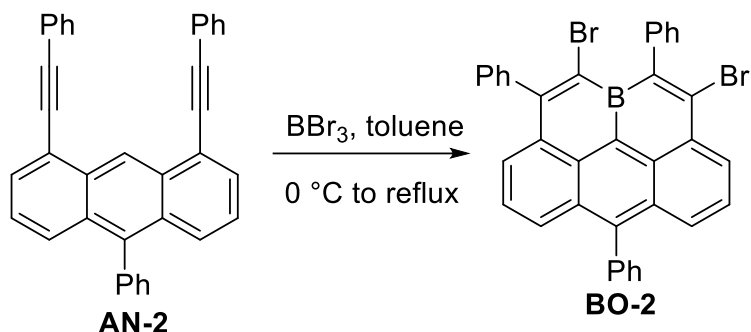
0.06 mmol, 0.1 equiv) were added under nitrogen atmosphere. The mixture was heated to 80 °C and monitored by TLC to confirm consumption of starting material. Upon completion, the resulting solution was washed with water, extracted with ethyl acetate and dried over anhydrous Na₂SO₄. After filtration and removal of the solvents, the crude product was purified by silica gel chromatography (eluent: petroleum ether/CH₂Cl₂ = 15:1) to give compound **5** as a orange solid in 82% yield (308 mg). ¹H NMR (400 MHz, CDCl₃): δ 9.73 (s, 1H), 8.15 (d, *J* = 8.9 Hz, 2H), 7.78 (d, *J* = 6.5 Hz, 2H), 7.59 (d, *J* = 7.3 Hz, 4H), 7.40 – 7.33 (m, 4H), 7.21 (t, *J* = 7.6 Hz, 4H), 7.15 (d, *J* = 8.3 Hz, 4H), 6.97 (d, *J* = 8.4 Hz, 4H), 1.25 (s, 18H); ¹³C NMR (100 MHz, CDCl₃): δ 145.18, 143.63, 138.80, 132.48, 131.82, 130.90, 130.64, 128.40, 128.33, 125.54, 123.22, 121.74, 119.53, 95.25, 87.54, 33.64, 31.38. MS (MALDI-TOF, m/z): calcd for C₅₀H₄₃N [M]⁺, 657.3396, found 657.3379, (error = -2.5 ppm).

2,11-dibromo-1,10-diphenyl-11a-boraolympicene (BO-1)



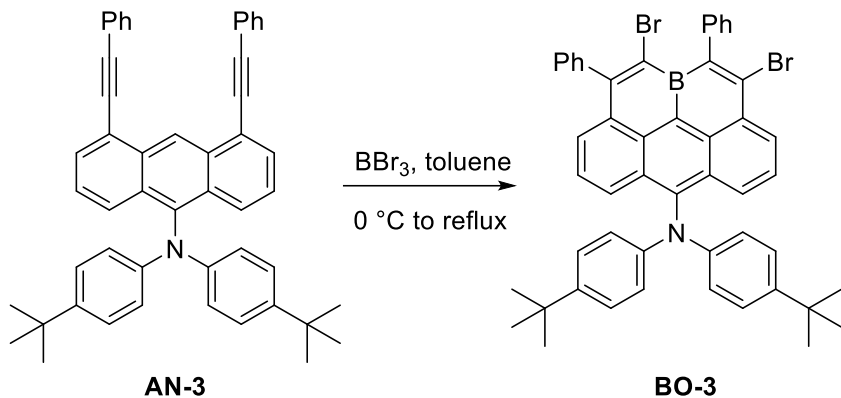
To a solution of 1,8-bis(phenylethynyl)anthracene **AN-1** (756 mg, 2.0 mmol, 1.0 equiv.) in anhydrous toluene, BBr₃ (2.0 mL, 1.0 M in hexane, 2.0 mmol, 1.0 equiv.) was added dropwise via a syringe at 0 °C under an argon atmosphere. The mixture was kept stirring at 0 °C for about 0.5 h, and then heated to reflux. The reaction was monitored by TLC to confirm consumption of starting material. Upon completion, the resulting solution was cooled down to room temperature and then quenched with water, extracted with CH₂Cl₂ and dried over anhydrous Na₂SO₄. After filtration and removal of the solvents, the crude product was purified by silica gel chromatography (eluent: petroleum ether/CH₂Cl₂ = 10:1) to give compound **BO-1** as a red solid in 45% yield (491 mg). ¹H NMR (400 MHz, CDCl₃): δ 9.26 – 9.20 (m, 2H), 8.53 (d, *J* = 7.5 Hz, 1H), 8.44 (d, *J* = 7.1 Hz, 1H), 7.98 – 7.93 (t, *J* = 7.9 Hz, 1H), 7.83 (d, *J* = 7.3 Hz, 1H), 7.67 (t, *J* = 7.3 Hz, 1H), 7.51 – 7.39 (m, 6H), 7.38 – 7.28 (m, 4H); ¹³C NMR (100 MHz, CDCl₃): δ 157.34, 146.67, 142.94, 142.54, 140.71, 140.46, 140.22, 138.77, 138.71, 135.05, 134.86, 134.34, 134.30, 131.79, 129.75, 129.14, 128.22, 127.74, 127.34, 126.50, 126.38, 126.21, 125.21, 119.60; ¹¹B NMR (128 MHz, CDCl₃): δ 42.3; HR-MS (MALDI-TOF) *m/z*: Calcd for C₃₀H₁₇BBr₂ [M]⁺: 547.9770, Found: 547.9762 (error = -1.4 ppm).

2,11-dibromo-1,6,10-triphenyl-11a- boraolympicene (BO-2)



Compound **BO-2** was synthesized in 52% yield as a red solid, a similar synthetic process to **BO-1**. ^1H NMR (400 MHz, CDCl_3): δ 9.20 (d, $J = 6.6$ Hz, 1H), 8.17 (d, $J = 8.5$ Hz, 1H), 8.08 (d, $J = 8.8$ Hz, 1H), 7.81 – 7.76 (m, 2H), 7.70 – 7.58 (m, 4H), 7.57 – 7.54 (m, 2H), 7.43 (m, 5H), 7.36 – 7.29 (m, 5H); ^{13}C NMR (100 MHz, CDCl_3): δ 157.53, 152.34, 148.35, 143.11, 140.38, 138.55, 133.54, 131.78, 131.70, 131.44, 129.97, 129.74, 129.21, 129.06, 128.49, 127.81, 127.73, 127.31, 126.20, 126.06; ^{11}B NMR (128 MHz, CDCl_3): δ 43.2; HR-MS (MALDI-TOF) m/z : Calcd for $\text{C}_{36}\text{H}_{21}\text{BBr} [\text{M}]$: 624.0083, Found: 624.0078 (error = -0.8 ppm).

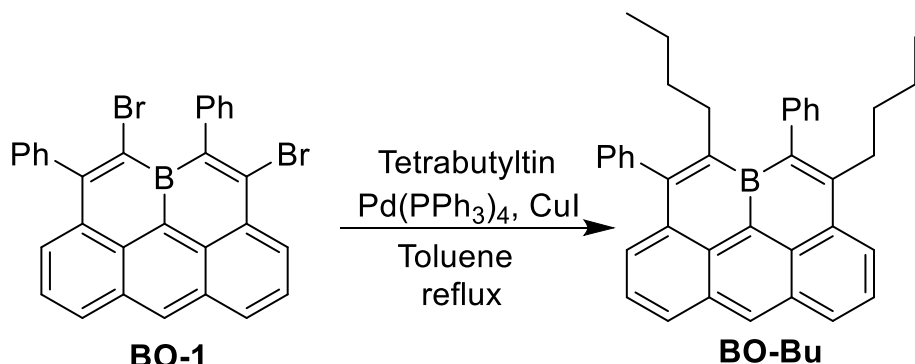
2,11-dibromo-N,N-bis(4-(tert-butyl)phenyl)-1,10-diphenyl-11a-boraolympicene-6-amine (BO-3)



Compound **BO-3** was synthesized in 67% yield as a dark green solid, a similar synthetic process to **BO-1**. ^1H NMR (400 MHz, CD_2Cl_2): δ 9.08 (d, $J = 7.4$ Hz, 1H), 8.68 (d, $J = 8.5$ Hz, 1H), 8.57 (d, $J = 8.5$ Hz, 1H), 7.75 (t, $J = 8.0$ Hz, 1H), 7.66 (d, $J = 7.3$ Hz, 1H), 7.43 (m, $J = 7.8$, 7.4 Hz, 6H), 7.35 (d, $J = 7.0$ Hz, 1H), 7.32 – 7.26 (m, 4H), 7.24 (d, $J = 8.8$ Hz, 4H), 7.03 (d, $J = 8.7$ Hz, 4H), 1.26 (s, 18H); ^{13}C NMR (100 MHz, CD_2Cl_2): δ 158.54, 153.27, 148.19, 147.14, 145.31, 143.54, 142.89, 140.53, 138.88, 135.55, 133.98, 133.02, 132.50, 131.61, 130.49, 130.35, 130.07, 129.63, 128.18, 128.07, 127.74, 127.50, 127.37, 126.71, 126.60, 121.48, 34.49,

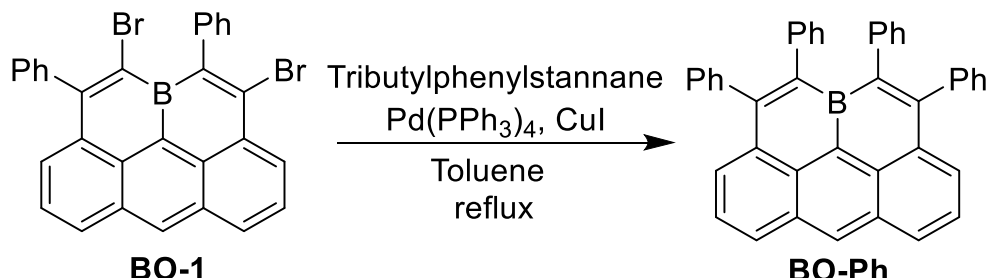
31.47; ^{11}B NMR (128 MHz, CDCl_3): δ 45.4; HR-MS (MALDI-TOF) m/z : Calcd for $\text{C}_{50}\text{H}_{42}\text{BBr}_2\text{N}$ [M]: 827.1757, Found: 827.1751 (error = -0.7 ppm).

1,10-dibutyl-2,11-diphenyl-11a-boraolympicene (BO-Bu)



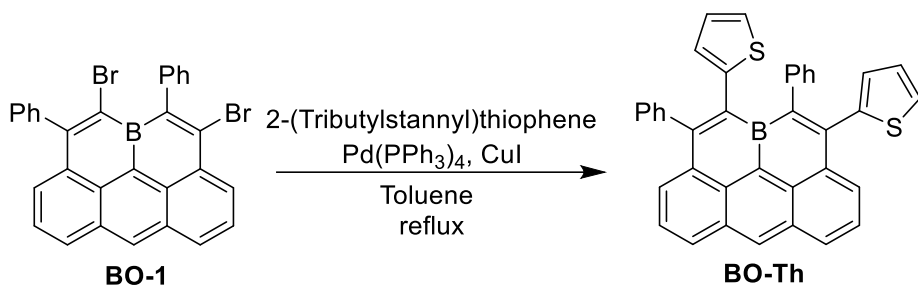
To a solution of compound **BO-1** (110 mg, 0.2 mmol, 1.0 equiv) in toluene (20 mL), Tetrabutyltin (208 mg, 0.6 mmol, 3.0 equiv), $\text{Pd}(\text{PPh}_3)_4$ (12 mg, 0.01 mmol, 0.05 equiv) and CuI (2 mg, 0.01 mmol, 0.05 equiv) were added under an argon atmosphere. The mixture was heated to 110 °C and monitored by TLC to confirm consumption of starting material. Upon completion, the resulting solution was washed with water, extracted with ethyl acetate and dried over anhydrous Na_2SO_4 . After filtration and removal of the solvents, the crude product was purified by silica gel chromatography (eluent: petroleum ether/ CH_2Cl_2 = 10:1) to give a reddish brown solid **BO-Bu** (86 mg) in 86 % yield. ^1H NMR (400 MHz, CDCl_3): δ 9.17 (s, 1H), 8.44 (m, 2H), 8.28 (d, J = 7.3 Hz, 1H), 8.15 (d, J = 7.8 Hz, 1H), 7.90 (t, J = 7.8 Hz, 1H), 7.73 (t, J = 6.6 Hz, 1H), 7.50 – 7.38 (m, 10H), 2.33 (m, 4H), 1.47 (m, 4H), 0.99 – 0.82 (m, 10H); ^{13}C NMR (100 MHz, CDCl_3): δ 157.14, 145.34, 144.23, 143.27, 138.81, 136.89, 136.70, 134.03, 133.79, 132.92, 130.16, 129.91, 128.38, 127.76, 127.12, 126.31, 126.13, 125.73, 37.93, 35.70, 35.28, 33.41, 28.69, 20.11, 19.72, 14.75; ^{11}B NMR (128 MHz, CDCl_3): δ 24.9; HR-MS (MALDI-TOF) m/z : Calcd for $\text{C}_{38}\text{H}_{35}\text{B}$ [M]: 502.2832, Found: 502.2830 (error = -0.4 ppm).

1,2,10,11-tetraphenyl-11a-11a-boraolympicene (BO-Ph)



Compound **BO-Ph** was synthesized in 85% yield as a red solid, a similar synthetic process to **BO-Bu**. ¹H NMR (400 MHz, CDCl₃): δ 9.25 (s, 1H), 8.43 (d, J = 8.2 Hz, 2H), 7.88 (d, J = 7.3 Hz, 2H), 7.70 (t, J = 7.7 Hz, 2H), 7.22 - 7.04 (m, 12H), 6.56 (broa, 8H); ¹³C NMR (100 MHz, CDCl₃): δ 144.26, 141.16, 139.52, 137.48, 134.53, 133.32, 131.10, 130.05, 129.60, 126.60, 126.26, 126.21, 126.02, 125.99, 125.92, 125.73, 123.49; ¹¹B NMR (128 MHz, CDCl₃): δ 29.5; HR-MS (MALDI-TOF) *m/z*: Calcd for C₄₂H₂₇B⁺[M]⁺: 542.2206; Found: 542.2238 (error = + 5.9 ppm). HR-MS (MALDI-TOF) *m/z*: Calcd for C₄₂H₂₇B [M]⁻: 542.2213, Found: 542.2238 (error = 4.6 ppm).

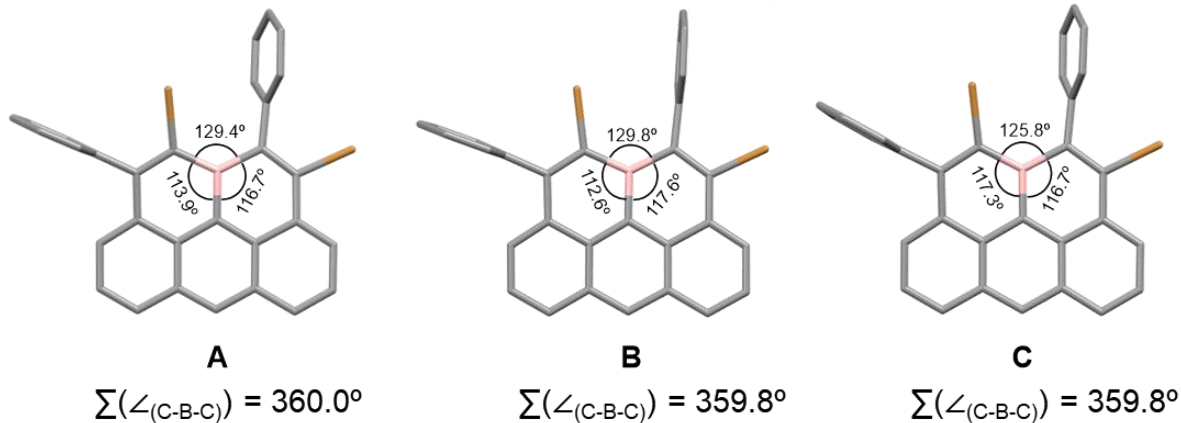
2,11-diphenyl-1,10-di(thiophen-2-yl)-11a- boraolympicene (BO-Th)



Compound **BO-Ph** was synthesized in 88% yield as a red solid, a similar synthetic process to **BO-Bu**. ¹H NMR (400 MHz, CDCl₃) δ 9.23 (s, 1H), 8.44 (d, J = 8.0 Hz, 2H), 8.18 (d, J = 7.2 Hz, 1H), 7.91 (d, J = 7.2 Hz, 1H), 7.78 - 7.69 (m, 2H), 7.29 - 7.17 (m, 7H), 6.90 - 6.88 (m, 1H), 6.82 (d, J = 3.3 Hz, 1H), 6.77 (d, J = 8.0 Hz, 4H), 6.63 (d, J = 5.1 Hz, 1H), 6.21 - 6.19 (m, 3.5 Hz, 1H), 6.00 (d, J = 3.3 Hz, 1H); ¹³C NMR (100 MHz, CDCl₃) δ 157.38, 146.80, 145.30, 144.54, 141.42, 140.82, 139.90, 138.25, 137.47, 134.67, 134.19, 133.95, 133.68, 130.96, 130.13, 129.98, 129.96, 129.95, 129.66, 128.90, 127.99, 127.15, 126.66, 126.40, 126.29, 126.17, 126.03, 126.01, 125.56, 125.53, 123.80, 123.27; ¹¹B NMR (128 MHz, CDCl₃): δ 28.4; HRMS (APCI) *m/z*: Calcd for C₃₈H₂₃BS₂ [M]⁻: 554.1334; Found: 554.1311(error = - 4.2 ppm).

3. Single-crystal X-Ray analysis

(a) BO-1



(b) BO-2

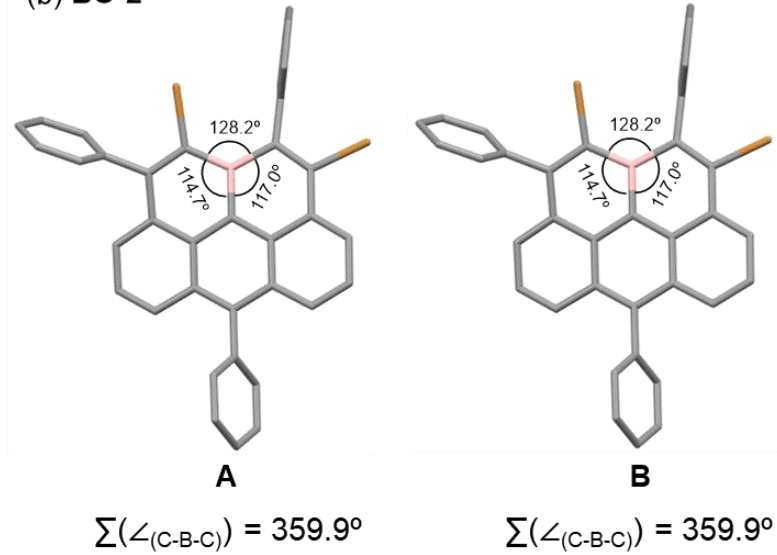


Figure S1. C–B–C angles ($\angle_{(C-B-C)}$) in the crystal structure of (a) BO-1 and (b) BO-2.

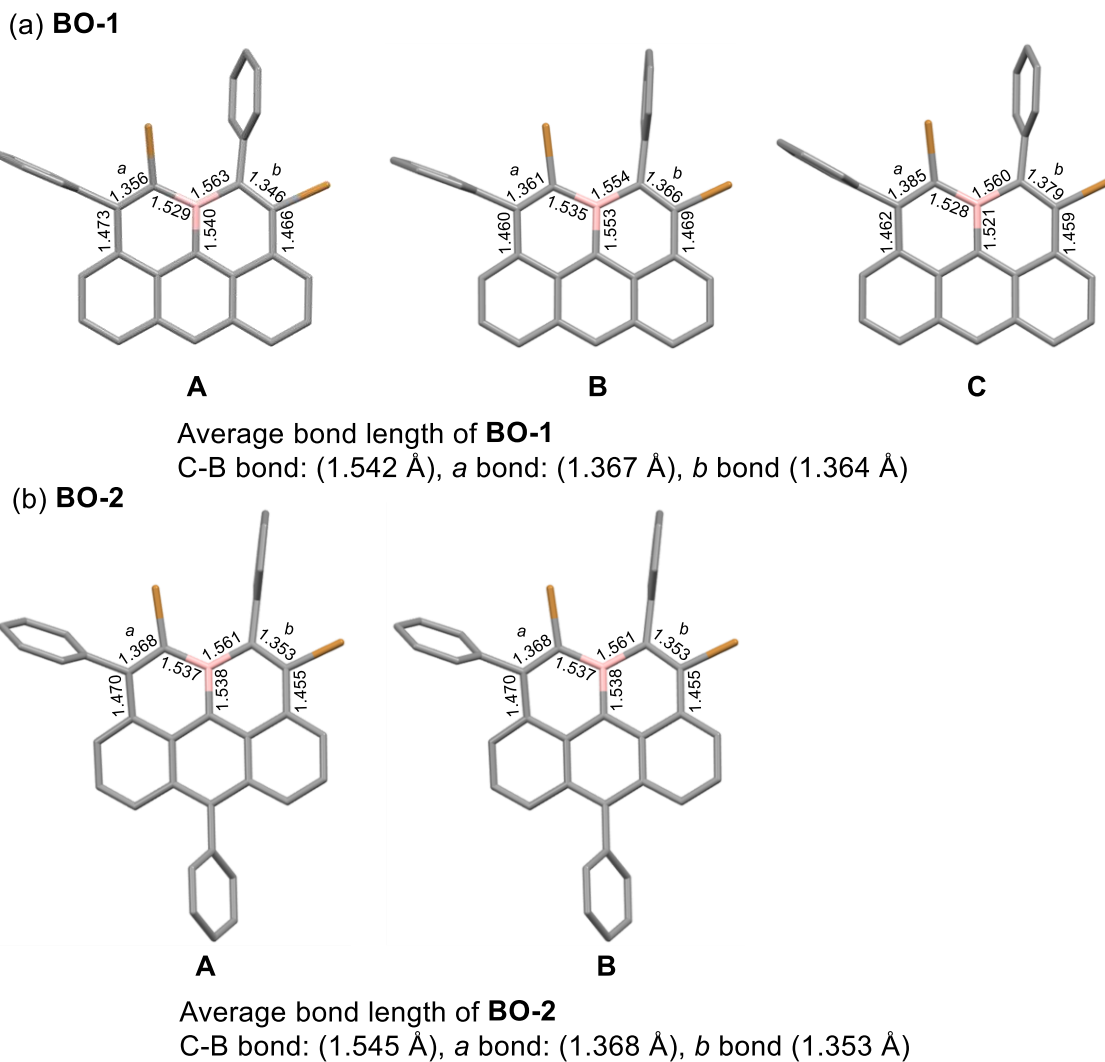


Figure S2. Selected bond length in the crystal structure of (a) **BO-1** and (b) **BO-2**.

4 TD-DFT simulations of 11a-boraolympicenes

DFT calculations and time-dependent DFT (TD-DFT) simulations were performed using the Gaussian 09 software package^[S1]. The geometries of all molecules were optimized at the B3LYP/6-31G(d,p) level, and energies were calculated at the same level of theory. TD-DFT calculations were conducted at the B3LYP/6-31G(d,p) level.

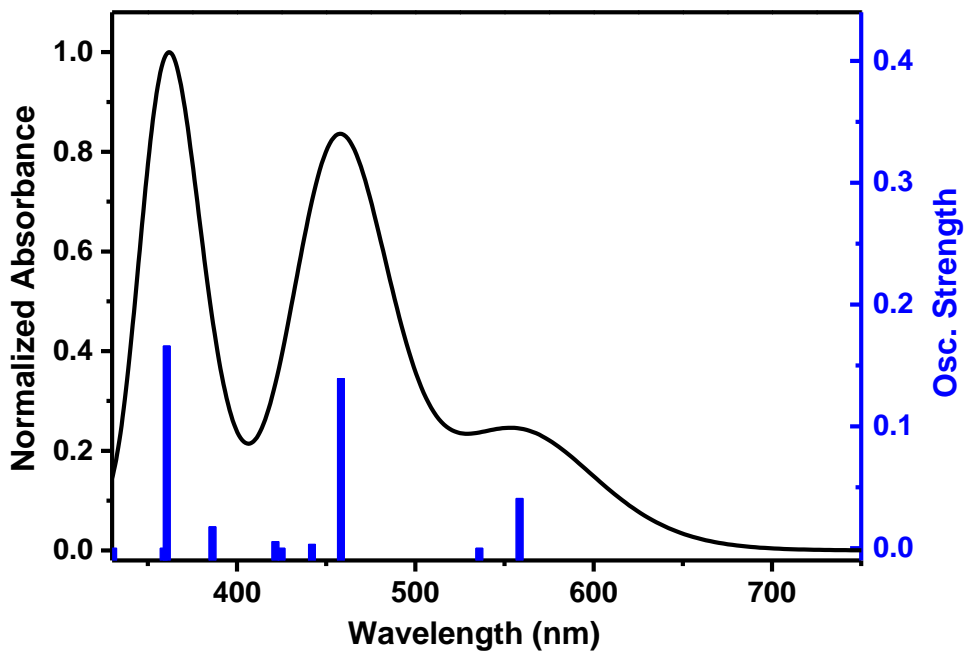


Figure S3. Calculated (B3LYP/6-31G(d,p)) absorption spectrum of **BO-1**.

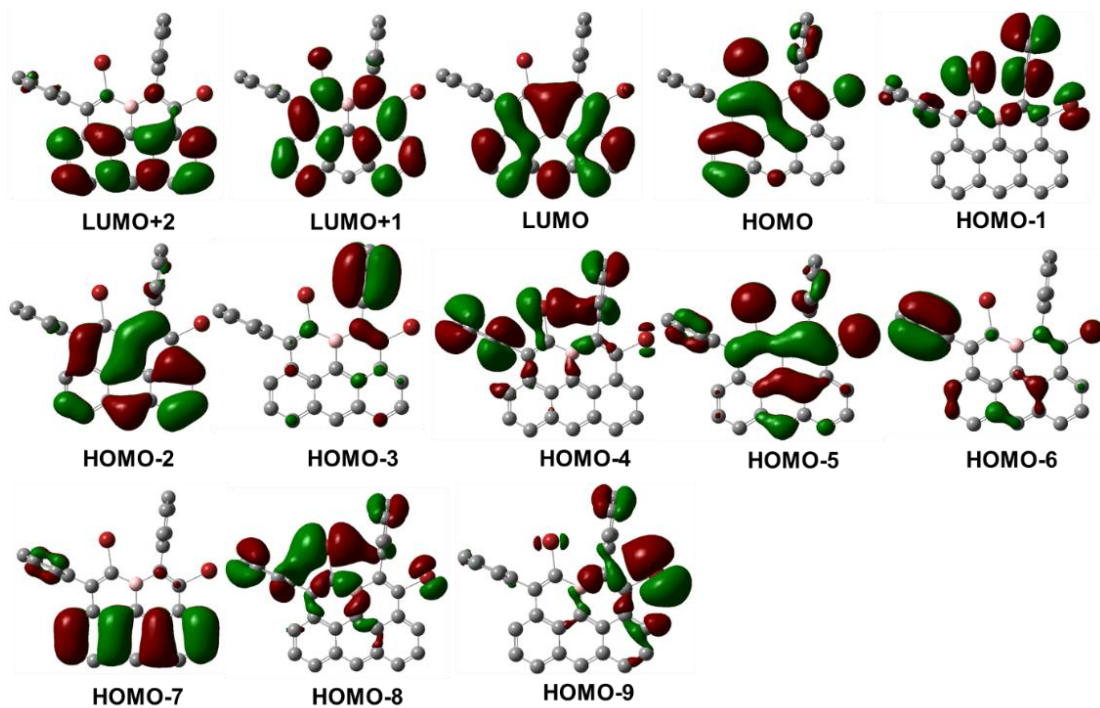


Figure S4. Calculated MOs profiles of **BO-1** at the B3LYP/6-31G(d,p) level.

Major electronic transitions of **BO-1** calculated by TD-DFT.

Excited State	Energy (eV)	Wavelength (nm)	Osc. Strength	Description

1	2.22	558.43	0.0409	HOMO→LUMO (90%)
2	2.31	535.91	0.0001	HOMO-1→LUMO (99%)
3	2.71	458.30	0.1393	HOMO-2→LUMO (89%)
4	2.80	442.07	0.0032	HOMO-3→LUMO (94%)
5	2.92	424.95	0.0001	HOMO-4→LUMO (98%)
6	2.94	421.58	0.0055	HOMO-5→LUMO (93%)
7	3.21	386.28	0.0177	HOMO-6→LUMO (97%)
8	3.44	360.63	0.1660	HOMO-7→LUMO (83%)
9	3.45	358.95	0.0000	HOMO-8→LUMO (97%)
10	3.75	330.58	0.0000	HOMO-9→LUMO (97%)
11	3.95	313.99	0.0043	HOMO-10→LUMO (94%)
12	4.10	302.63	0.0000	HOMO-11→LUMO (89%)
13	4.16	298.34	0.0002	HOMO-1→LUMO+1 (90%)
14	4.21	294.76	0.1311	HOMO→LUMO+1 (84%), HOMO-12→LUMO (54%),
15	4.34	285.59	0.0283	HOMO-2→LUMO+1 (28%), HOMO→LUMO+3 (13%)

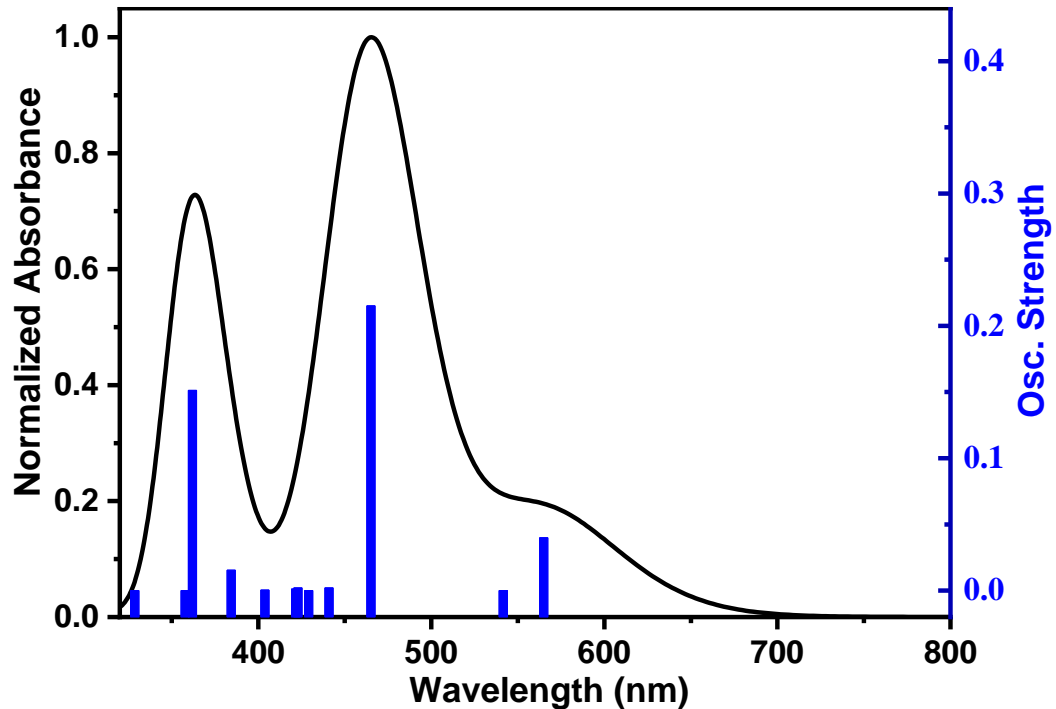


Figure S5. Calculated (B3LYP/6-31G(d,p)) absorption spectrum of **BO-2**.

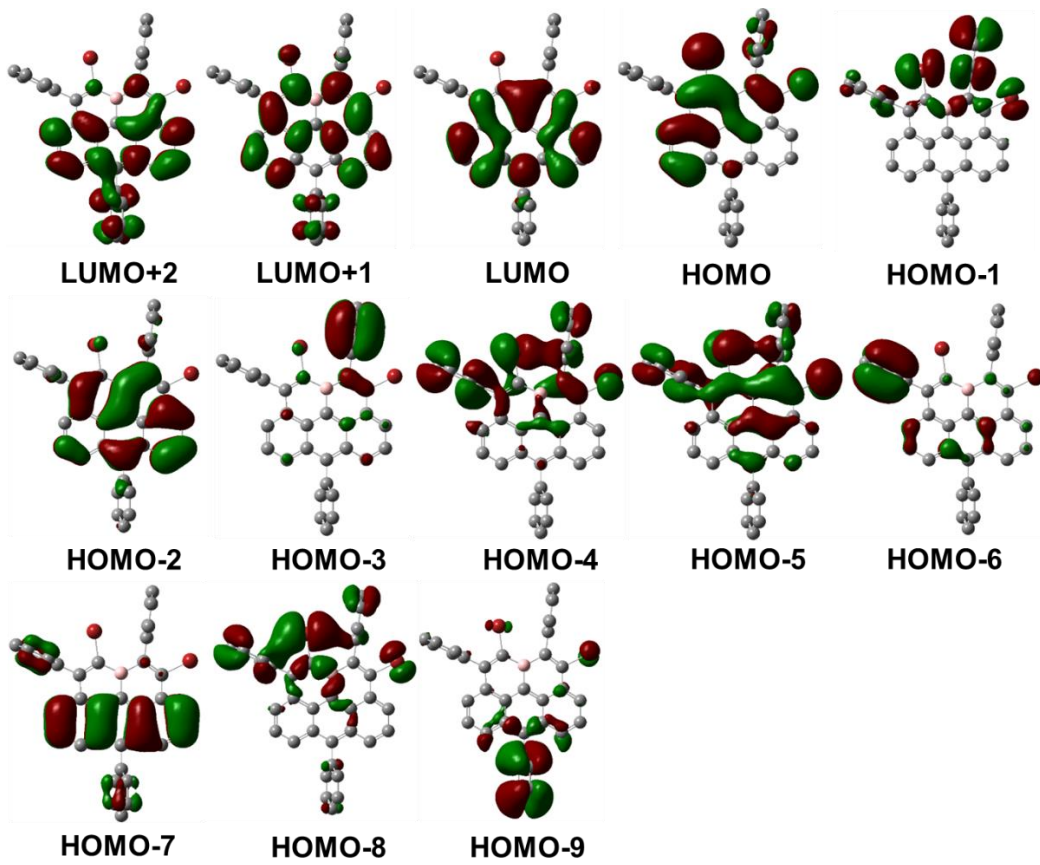


Figure S6. Calculated MOs profiles of **BO-2** at the B3LYP/6-31G(d,p) level.

Major electronic transitions of **BO-2** calculated by TD-DFT.

Excited State	Energy (eV)	Wavelength (nm)	Osc. Strength	Description
1	2.19	564.93	0.0400	HOMO→LUMO (90%)
2	2.29	541.58	0.0000	HOMO-1→LUMO (99%)
3	2.67	465.09	0.2152	HOMO-2→LUMO (89%)
4	2.81	440.86	0.0021	HOMO-3→LUMO (93%)
5	2.89	429.11	0.0000	HOMO-6→LUMO (68%), HOMO-4→LUMO (30%), HOMO-4→LUMO (41%),
6	2.93	422.94	0.0020.	HOMO-5→LUMO (39%), HOMO-6→LUMO (14%) HOMO-5→LUMO (53%),
7	2.94	421.61	0.0012	HOMO-4→LUMO (27%), HOMO-6→LUMO (17%)
8	3.07	403.86	0.0004	HOMO-7→LUMO (99%)
9	3.23	384.39	0.0155	HOMO-8→LUMO (98%)

10	3.43	361.98	0.1513	HOMO-9→LUMO (84%)
11	3.47	357.72	0.0000	HOMO-10→LUMO (97%)
12	3.77	328.61	0.0000	HOMO-11→LUMO (97%)
13	3.94	314.42	0.0014	HOMO-12→LUMO (95%)
14	4.07	304.46	0.0000	HOMO-13→LUMO (92%)
15	4.16	298.06	0.0001	HOMO-1→LUMO+1 (94%)

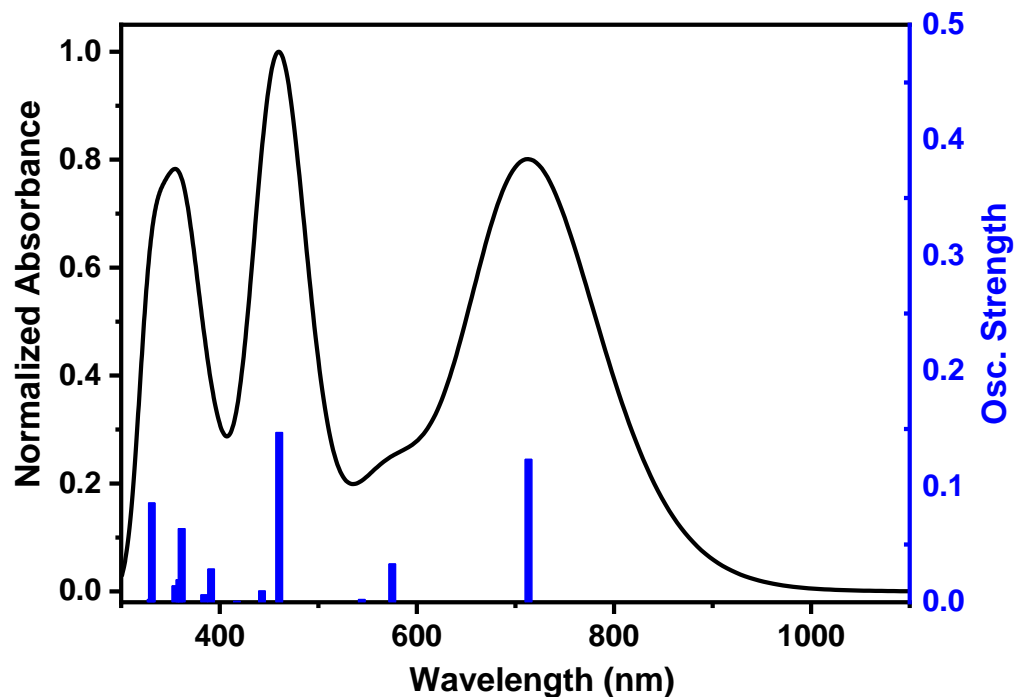


Figure S7. Calculated (B3LYP/6-31G(d,p)) absorption spectrum of **BO-3**.

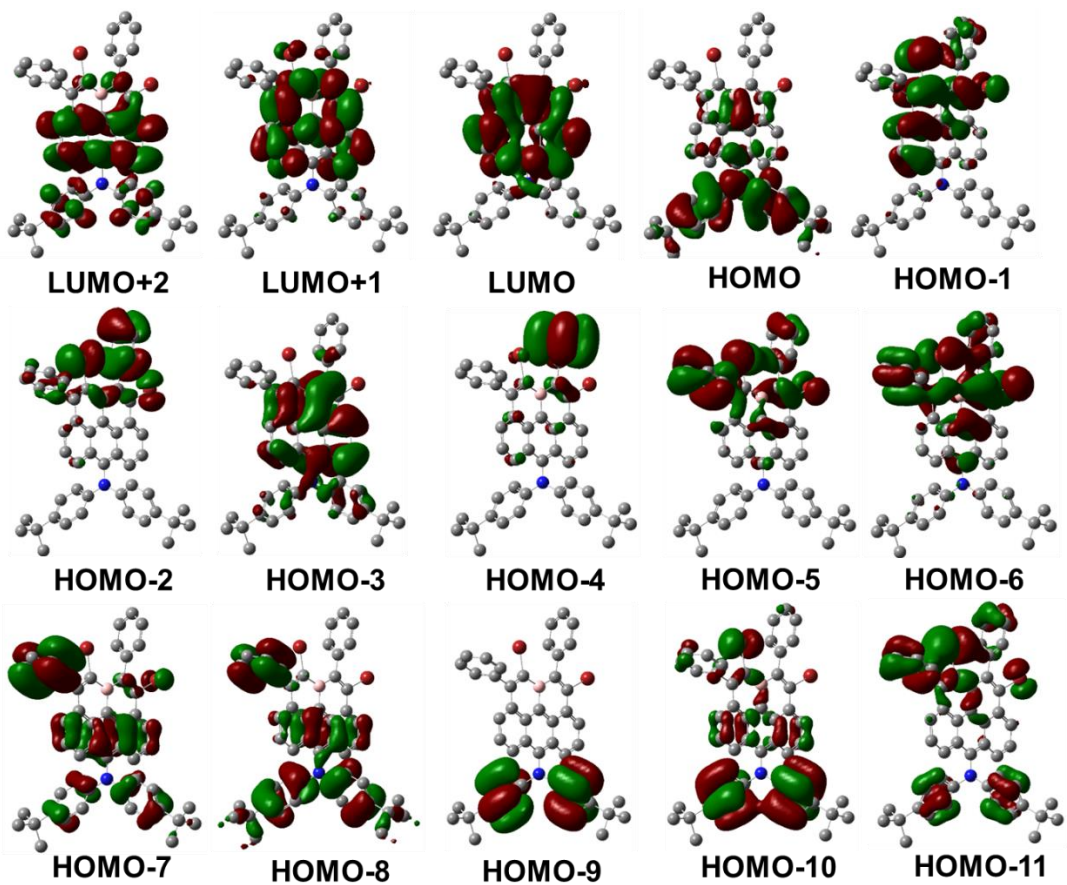


Figure S8. Calculated MOs profiles of **BO-3** at the B3LYP/6-31G(d,p) level.

Major electronic transitions of **BO-3** calculated by TD-DFT.

Excited State	Energy (eV)	Wavelength (nm)	Osc. Strength	Description
1	1.74	713.29	0.1238	HOMO→LUMO (98%)
2	2.16	575.07	0.0332	HOMO-1→LUMO (94%)
3	2.28	544.08	0.0025	HOMO-2→LUMO (99%)
4	2.69	460.31	0.1471	HOMO-3→LUMO (90%)
5	2.80	442.91	0.0099	HOMO-4→LUMO (91%)
6	2.88	430.04	0.0000	HOMO-5→LUMO (93%)
7	2.97	417.37	0.0009	HOMO-6→LUMO (95%)
8	3.17	391.24	0.0288	HOMO-8→LUMO (18%), HOMO-7→LUMO (77%)
9	3.23	384.16	0.0000	HOMO-8→LUMO (80%), HOMO-7→LUMO (19%)
10	3.33	371.89	0.0064	HOMO-9→LUMO (99%)
11	3.43	361.40	0.0000	HOMO-10→LUMO (73%)

				HOMO-12→LUMO (60%),
12	3.45	359.17	0.0638	HOMO-11→LUMO (25%),
				HOMO-10→LUMO (10%)
13	3.49	355.03	0.0143	HOMO-12→LUMO (33%),
				HOMO-11→LUMO (63%)
14	3.75	331.04	0.0860	HOMO→LUMO+1 (88%)
15	3.76	329.90	0.0025	HOMO-13→LUMO (95%)

5. Additional photophysical properties of 11a-boraolympicenes

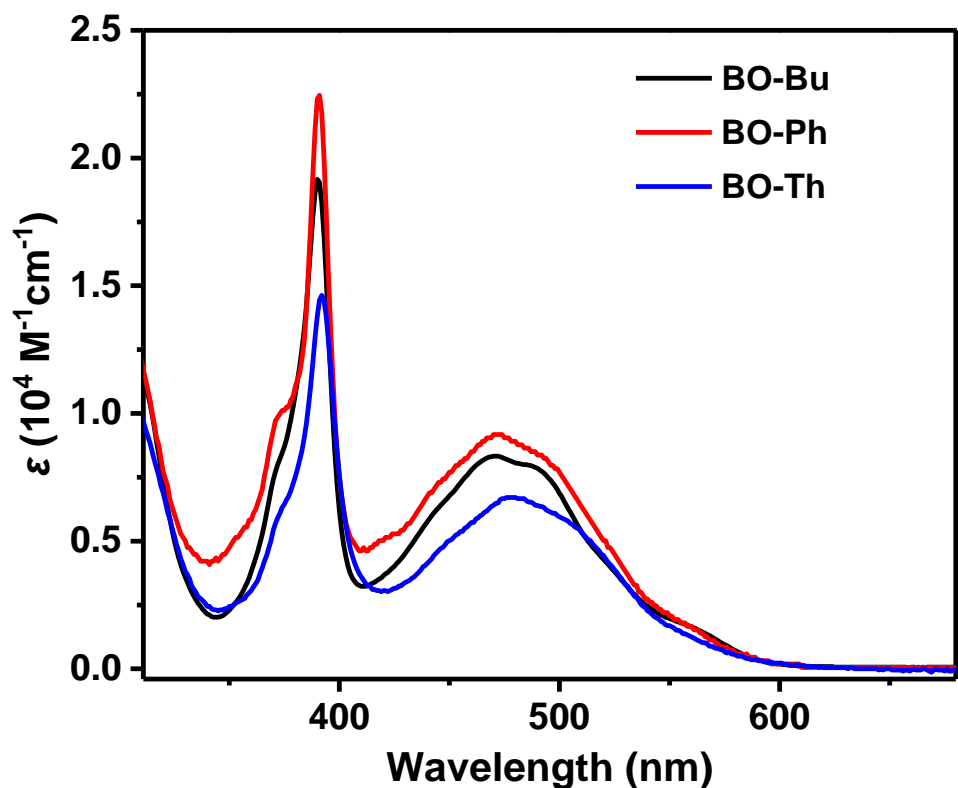


Figure S9. UV-vis-NIR absorption spectra of **BO-Bu**, **BO-Ph** and **BO-Th** recorded in DCM.

6 TD-DFT simulations of $(\text{BO}-2)^{-}$

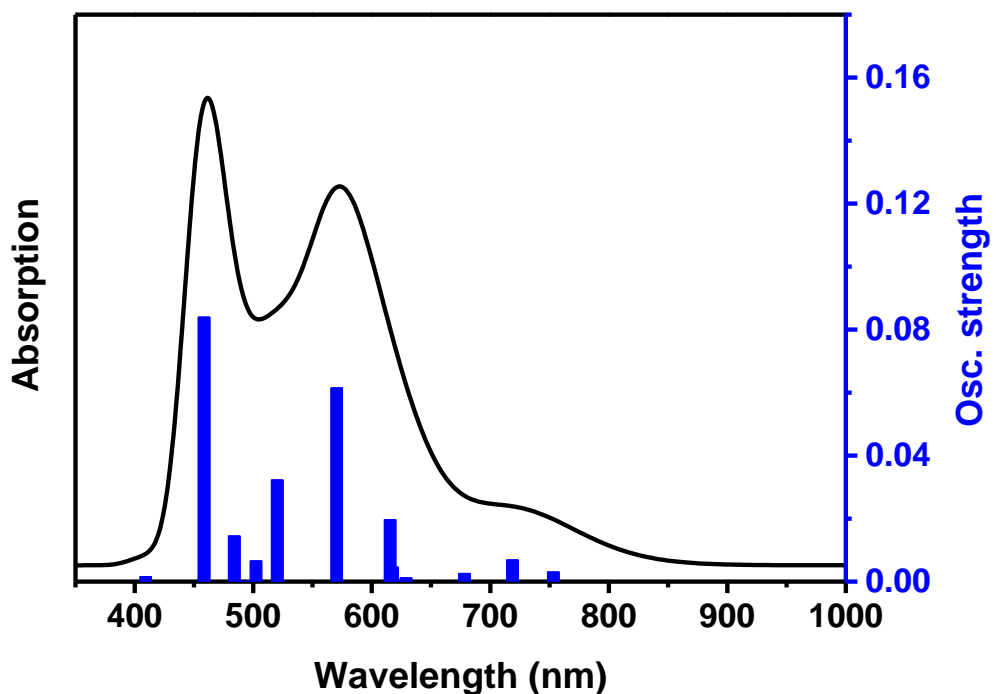


Figure S10. Calculated (UPBEPBE/6-31G(d,p)) absorption spectrum of $(\text{BO}-2)^{-}$.

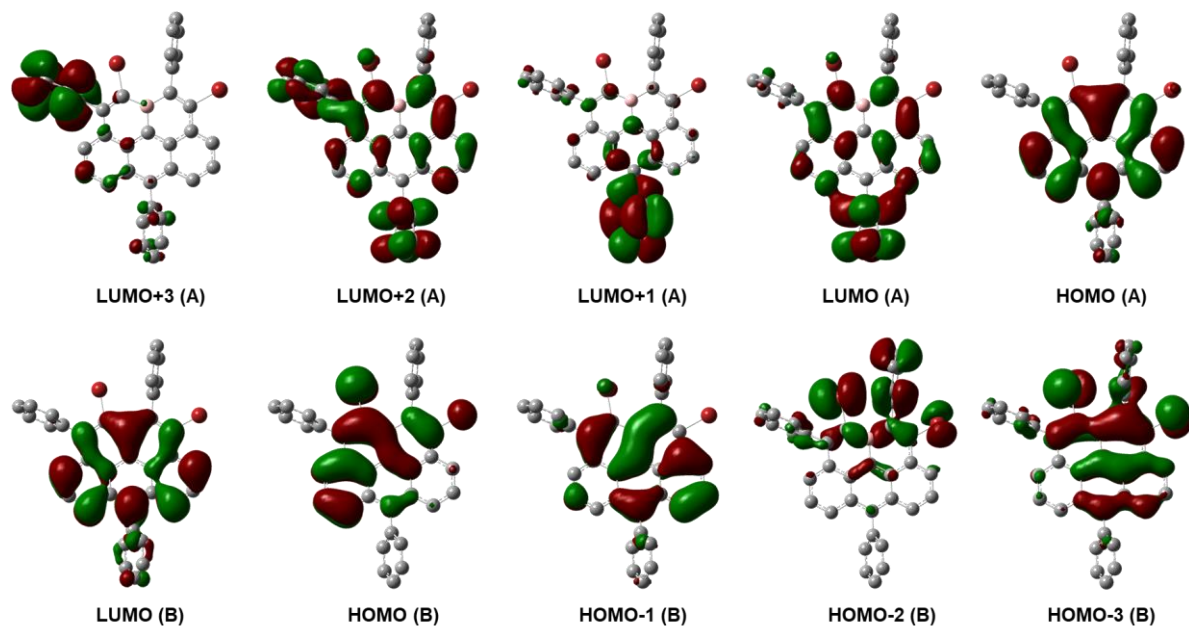


Figure S11. Calculated MOs profiles of $(\text{BO}-2)^{-}$ at the UPBEPBE/6-31G(d,p) level.

Major electronic transitions of $(\text{BO}-2)^{-}$ calculated by TD-DFT.

Excited State	Energy (eV)	Wavelength (nm)	Osc. Strength	Description
1	1.64549	753.15389	0.0031	HOMO(A) \rightarrow LUMO(A) (97%)
2	1.72446	718.66562	0.0069	HOMO(A) \rightarrow LUMO+1(A) (100%)

3	1.82742	678.17631	0.0026	HOMO(A)→LUMO+2(A) (32%), HOMO(B)→LUMO(B) (60%)
4	1.97046	628.94635	0.0012	HOMO(A)→LUMO+3(A) (72%), HOMO-1(B)→LUMO(B) (19%)
5	2.00674	617.57418	0.0046	HOMO(A)→LUMO+4(A) (84%)
6	2.01354	615.48944	0.0197	HOMO(A)→LUMO+2(A) (23%), HOMO(A)→LUMO+4(A) (15%), HOMO-1(B)→LUMO(B) (26%), HOMO(B)→LUMO(B) (20%)
7	2.17257	570.43567	0.0615	HOMO(A)→LUMO+2(A) (26%), HOMO(A)→LUMO+3(A) (21%), HOMO-1(B)→LUMO(B) (29%)
8	2.37898	520.94199	4E-4	HOMO(A)→LUMO+6(A) (99%)
9	2.38228	520.22067	0.0323	HOMO(A)→LUMO+5(A) (76%), HOMO(A)→LUMO+8(A) (15%)
10	2.46724	502.30601	0.0066	HOMO(A)→LUMO+7(A) (85%), HOMO-4(B)→LUMO(B) (10%)
11	2.51532	492.70463	1E-4	HOMO-2(B)→LUMO(B) (100%)
12	2.5607	483.97296	0.0145	HOMO(A)→LUMO+8(A) (14%), HOMO-3(B)→LUMO(B) (76%)
13	2.70304	458.48751	0.0840	HOMO(A)→LUMO+8(A) (61%), HOMO-3(B)→LUMO(B) (18%)
14	2.92924	423.08204	0	HOMO(A)→LUMO+9(A) (100%)
15	3.0282	409.25629	0.0016	HOMO-1(A)→LUMO(A) (20%), HOMO(B)→LUMO+1(B) (52%)

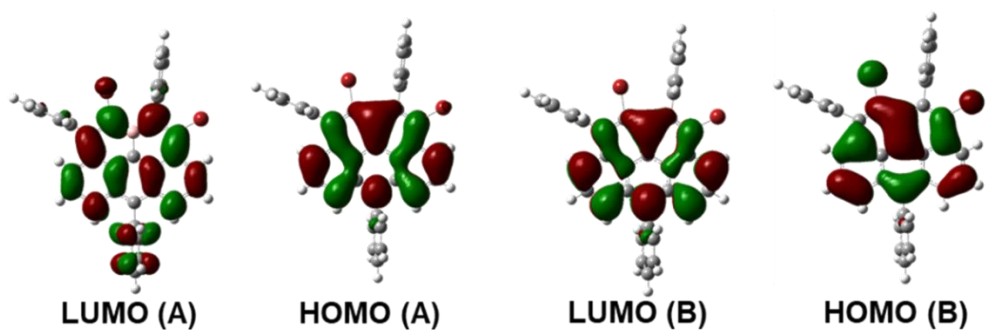


Figure S12. Calculated HOMOs and LUMOs profiles of **(BO-2)⁻** at the UB3LYP/6-31G(d,p) level.

7 FT-IR spectra of BO-2 and $(BO-2)^{-}$

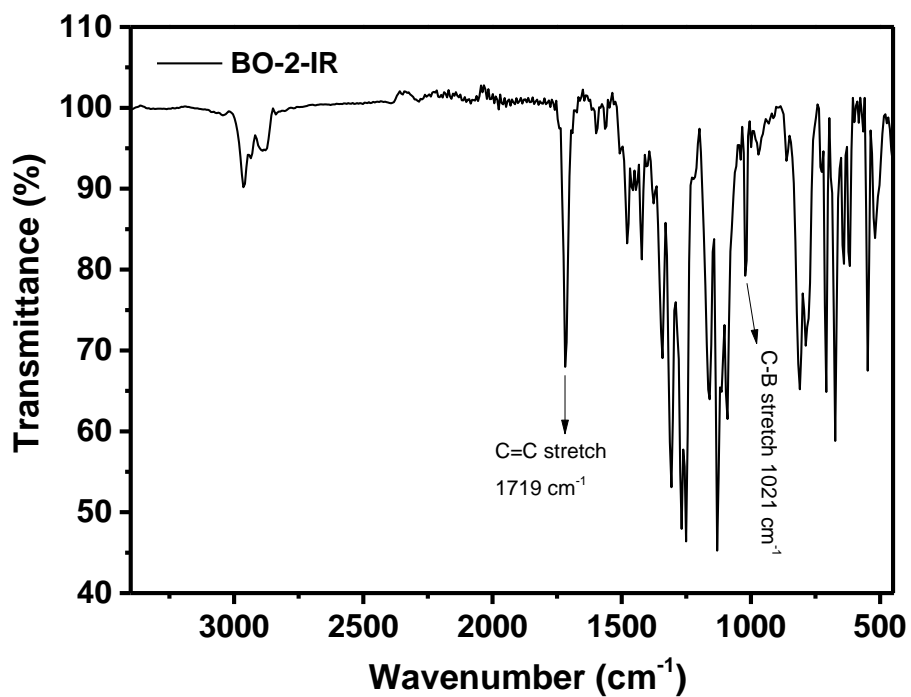


Figure S13. FT-IR spectra of BO-2.

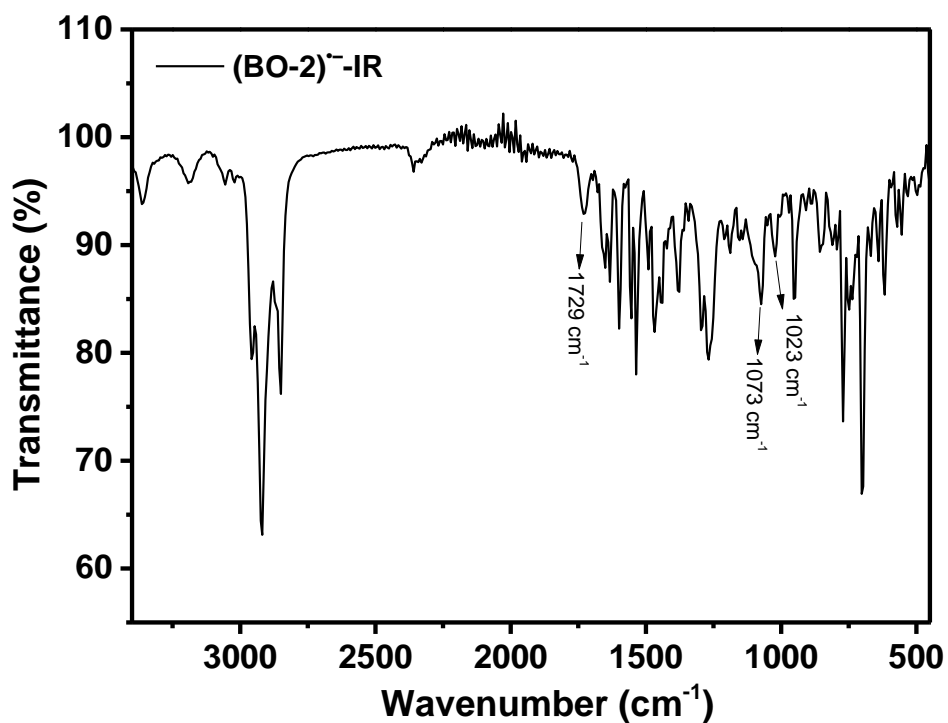
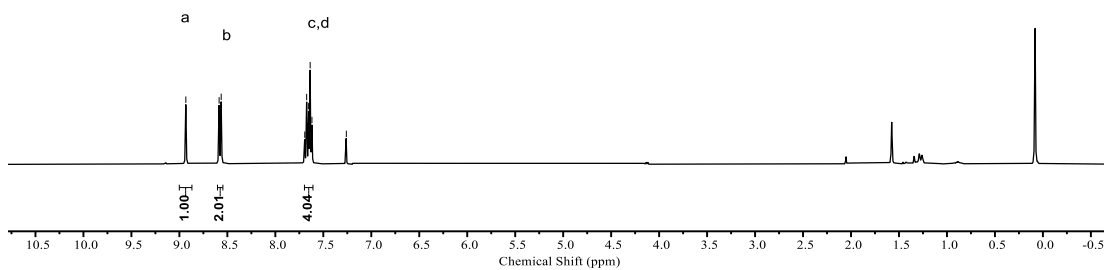
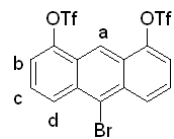


Figure S14. FT-IR spectra of $(BO-2)^{-}$.

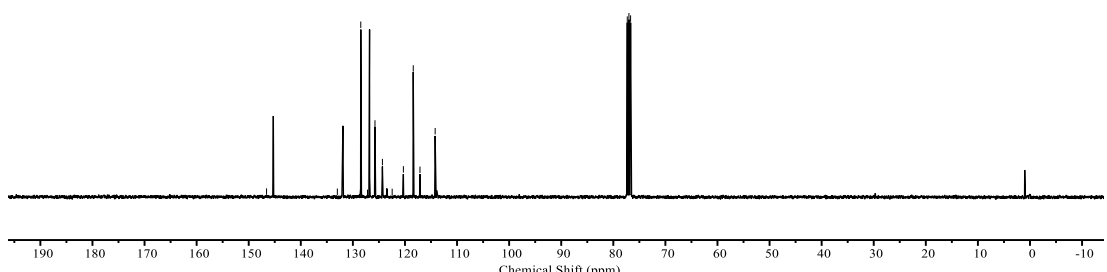
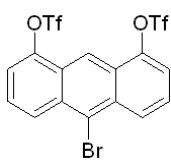
8. NMR and mass spectra of all new compounds

— 8.9328
 — 8.5860
 < 8.5645
 — 7.6932
 — 7.6735
 — 7.6530
 — 7.6370
 — 7.6184
 — 7.2600

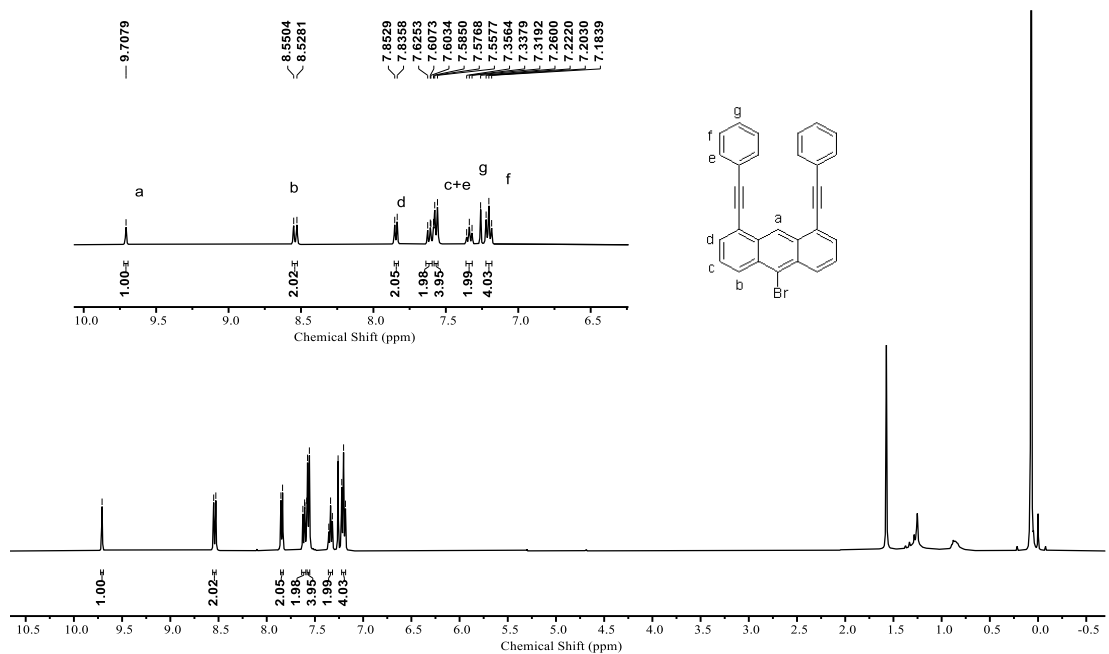


^1H NMR spectrum (400 MHz) of compound **2** in CDCl_3 at 298 K.

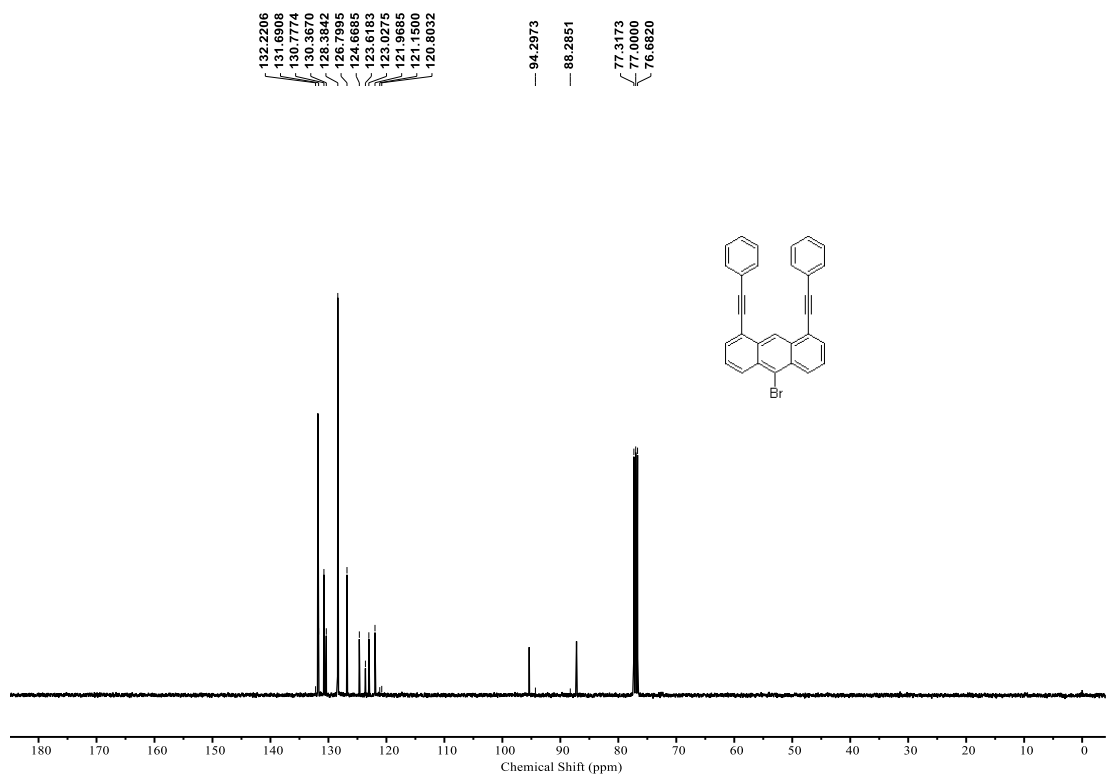
— 146.5739
 — 132.9831
 — 128.4844
 — 127.1950
 — 125.7594
 — 124.3302
 — 122.4567
 — 120.3024
 — 118.4093
 — 117.1178
 — 114.2033
 — 77.3476
 — 77.0000
 — 76.6827



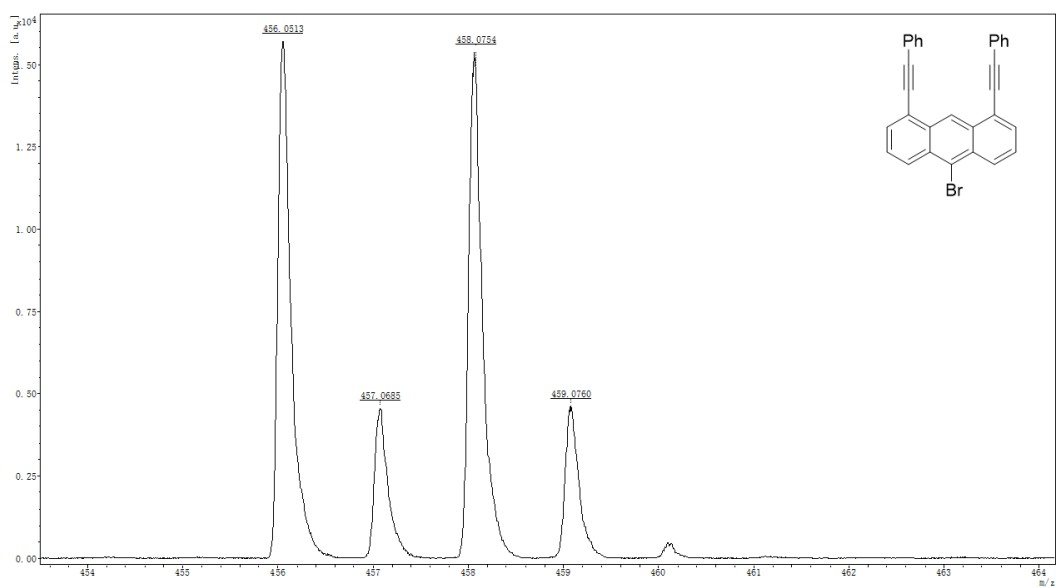
^{13}C NMR spectrum (100 MHz) of compound **2** in CDCl_3 at 298 K.



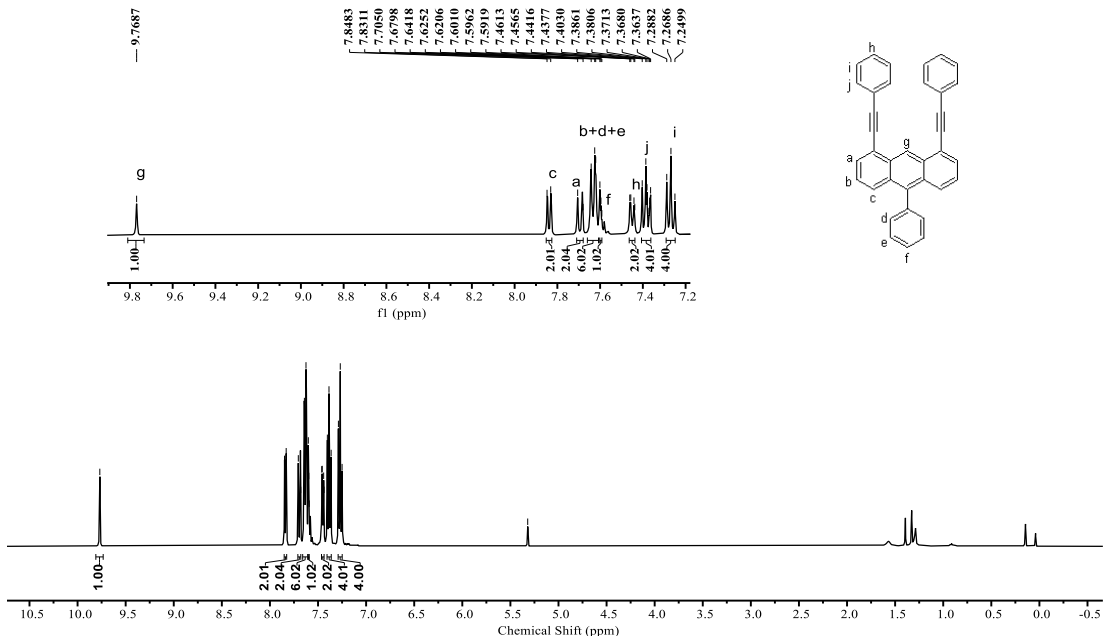
¹H NMR spectrum (400 MHz) of compound 3 in CDCl₃ at 298 K.



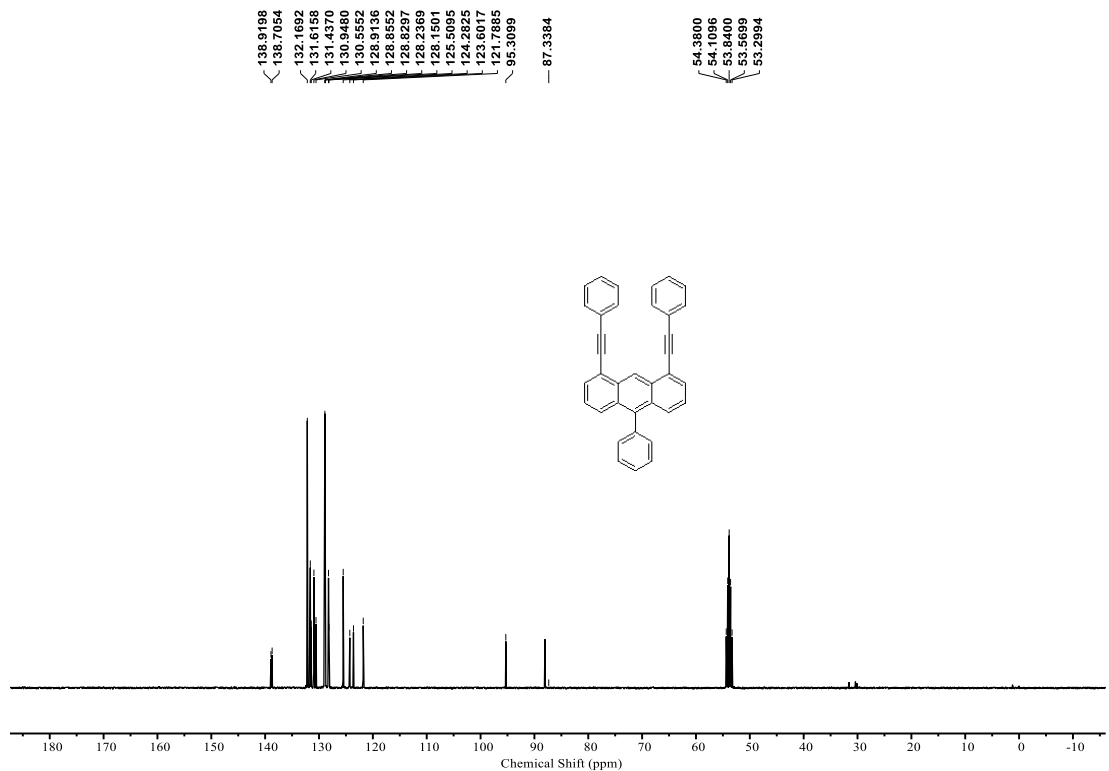
¹³C NMR spectrum (100 MHz) of compound 3 in CDCl₃ at 298 K.



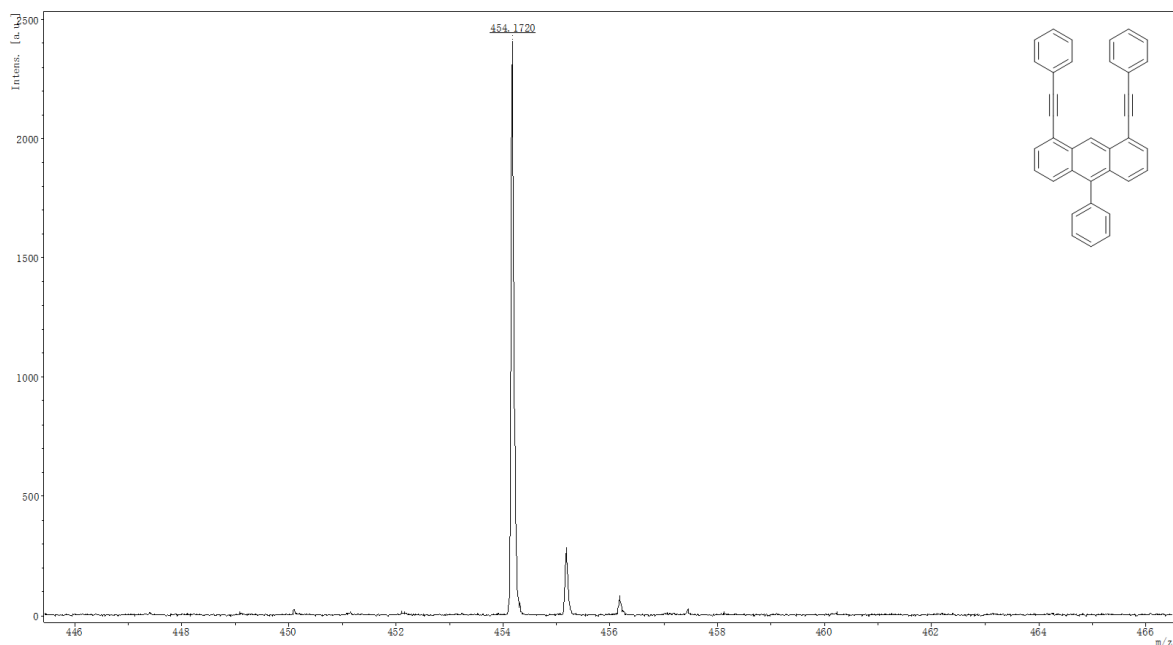
HR (MALDI-TOF) mass spectrum of compound **3**.



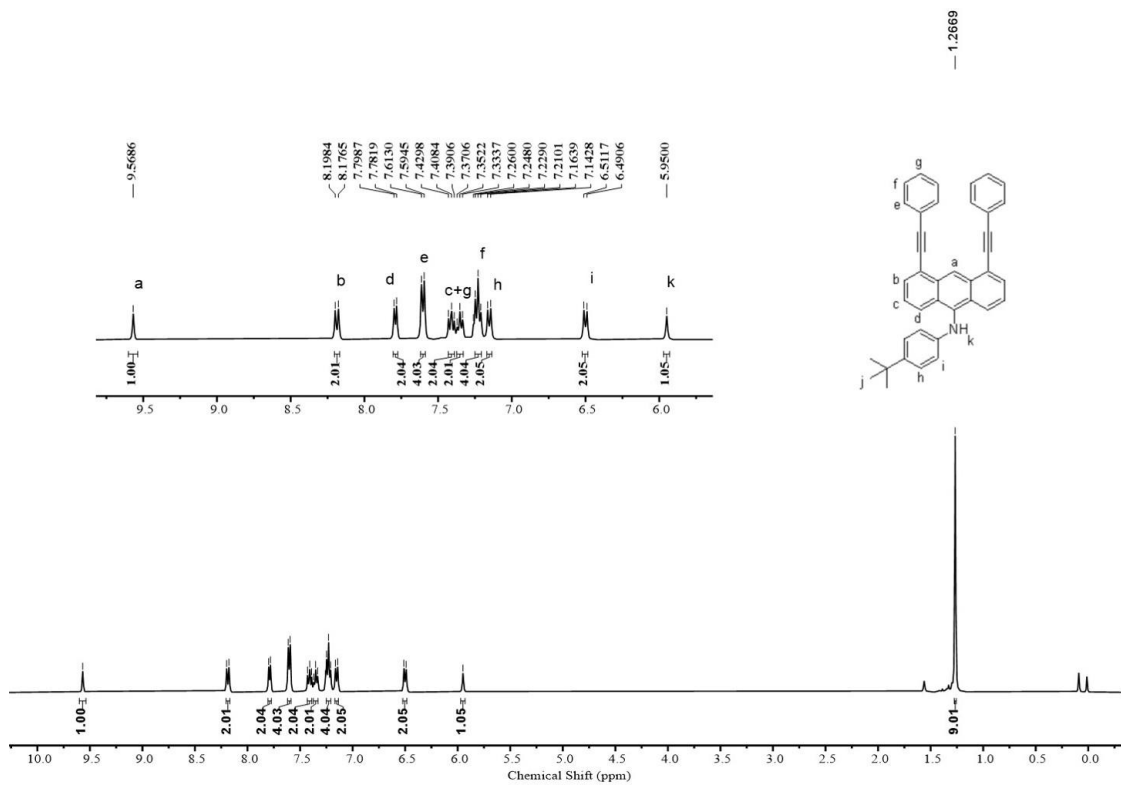
^1H NMR spectrum (400 MHz) of compound **AN-2** in CD_2Cl_2 at 298 K.



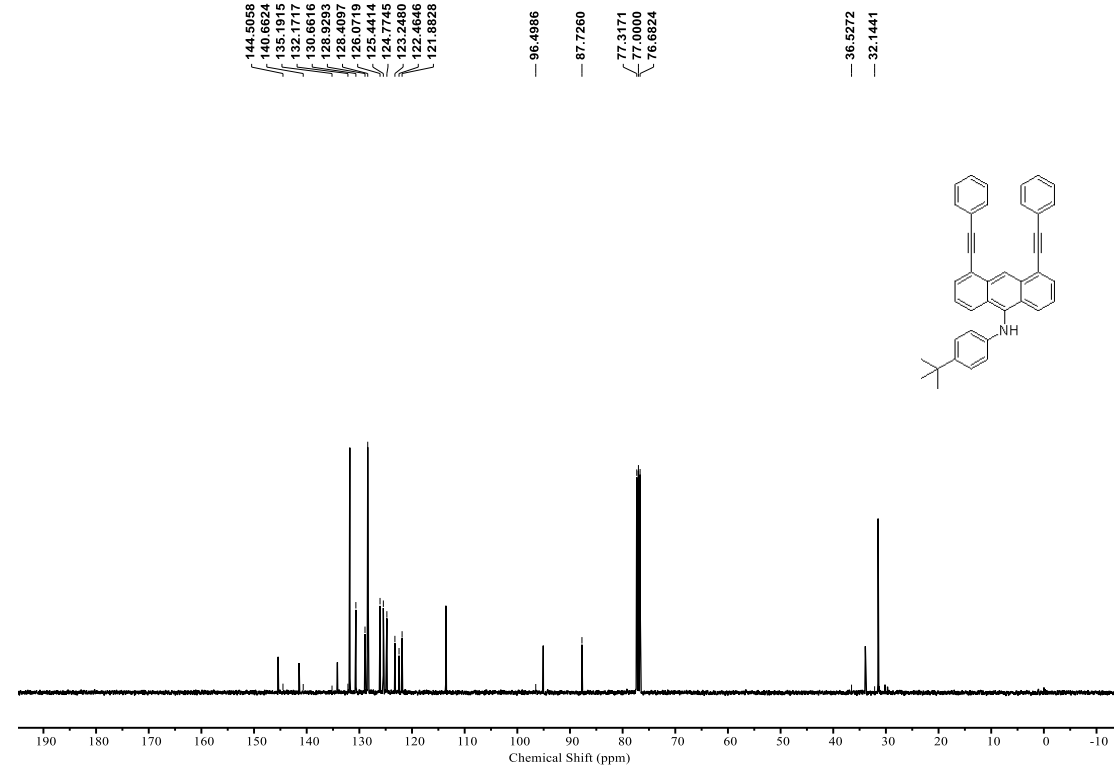
^{13}C NMR spectrum (100 MHz) of compound **AN-2** in CD_2Cl_2 at 298 K.



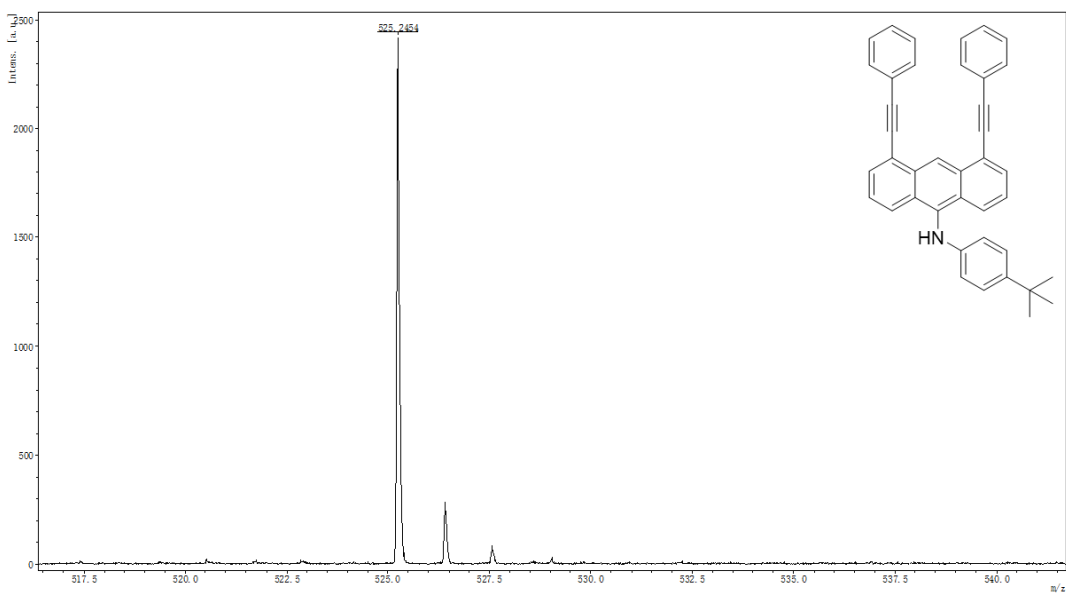
HR (MALDI-TOF) mass spectrum of compound **AN-2**.



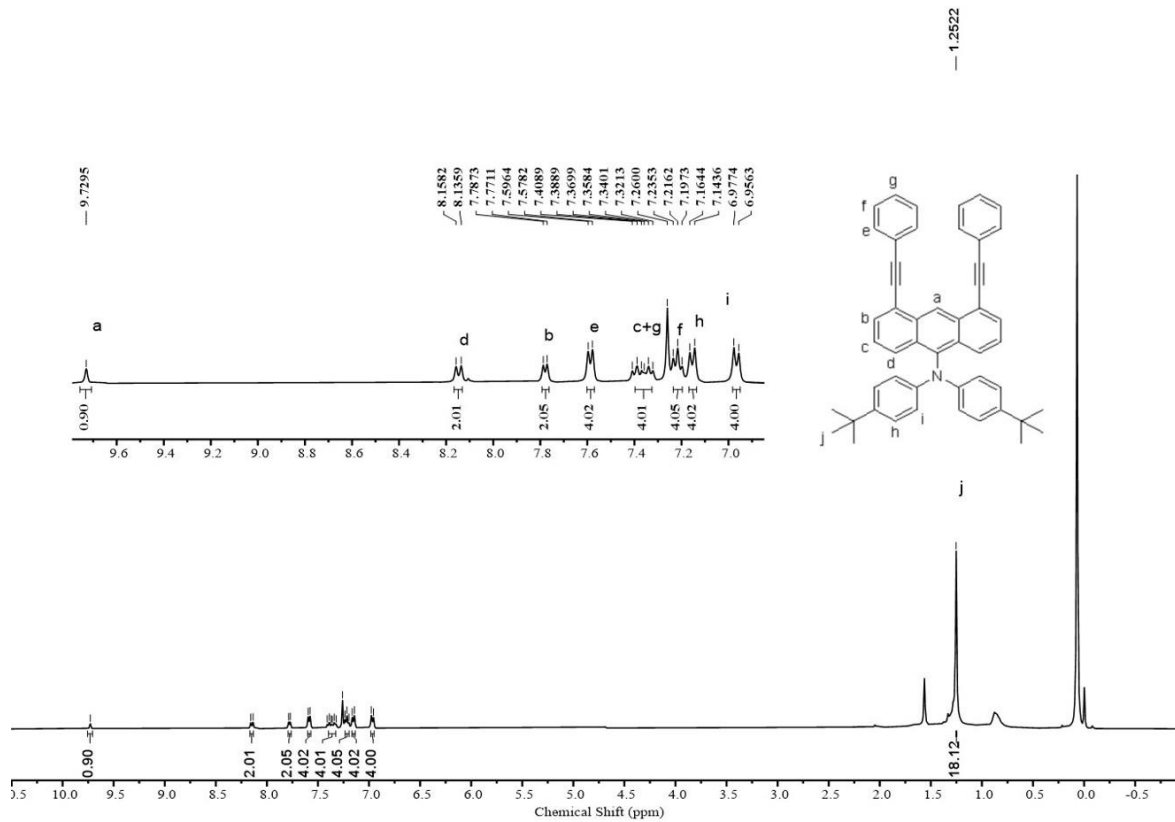
¹H NMR spectrum (400 MHz) of compound 4 in CDCl₃ at 298 K.

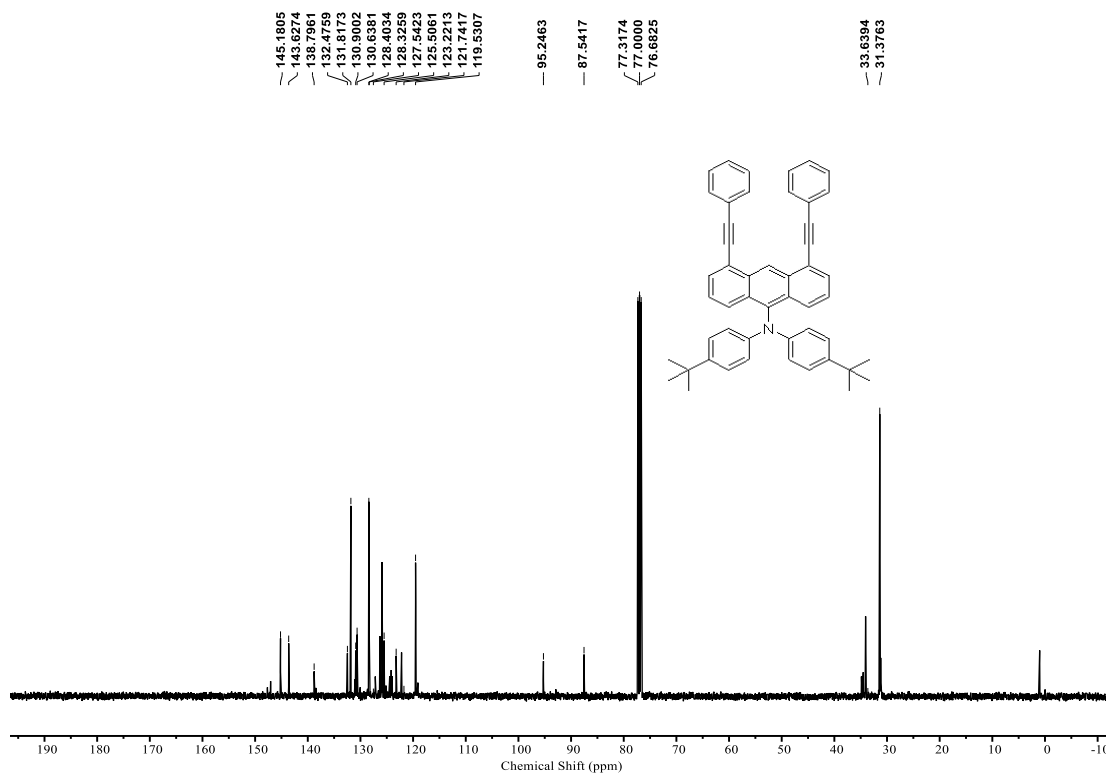


¹³C NMR spectrum (100 MHz) of compound 4 in CDCl₃ at 298 K.

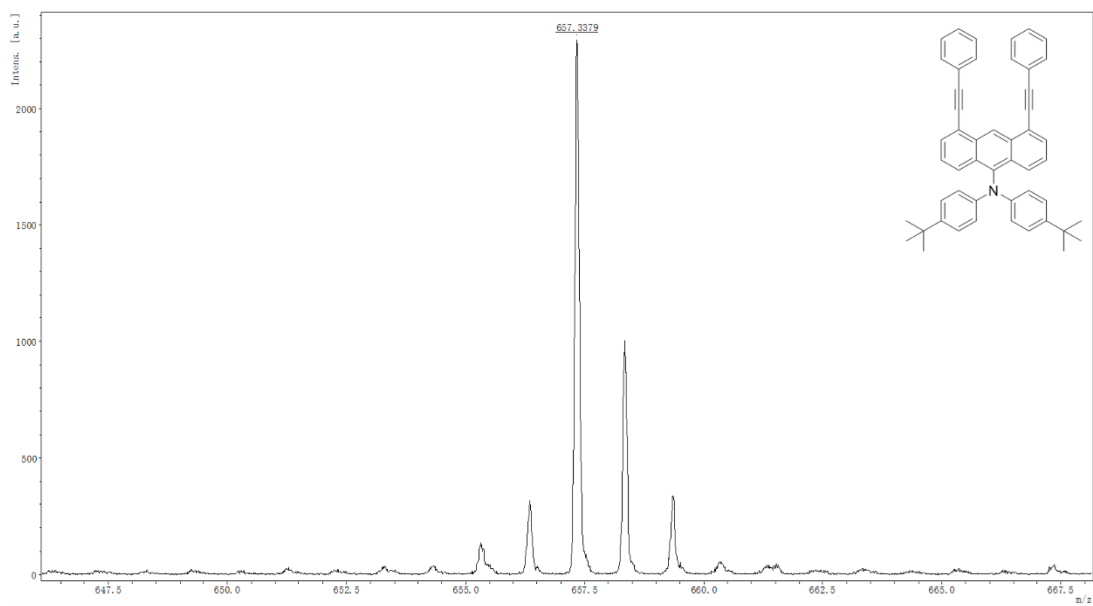


HR (MALDI-TOF) mass spectrum of compound **4**.

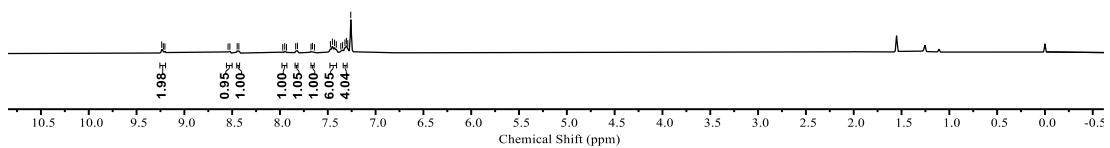
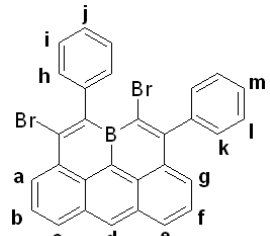
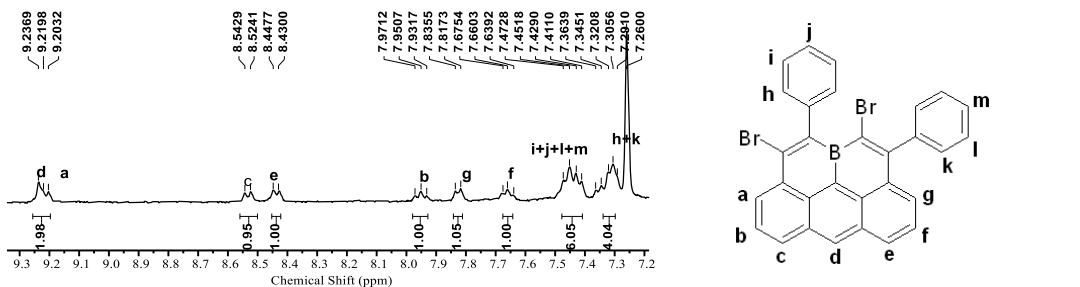




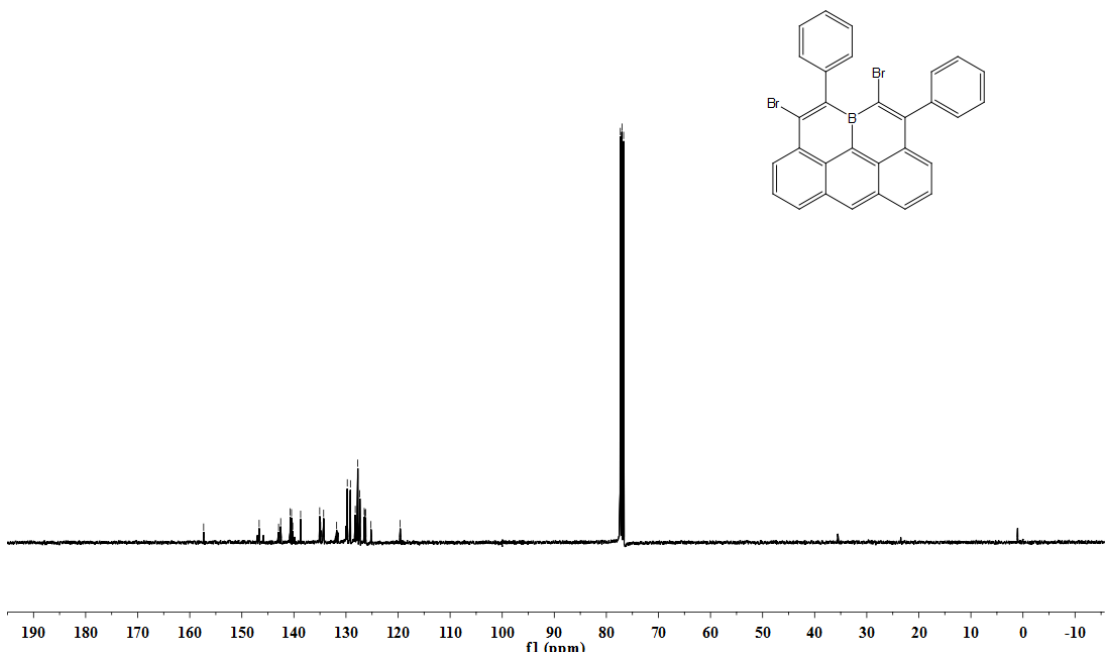
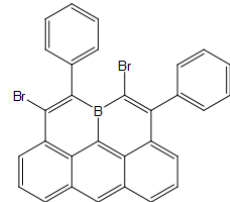
^{13}C NMR spectrum (100 MHz) of compound **AN-3** in CDCl_3 at 298 K.



HR (MALDI-TOF) mass spectrum of compound **AN-3**.

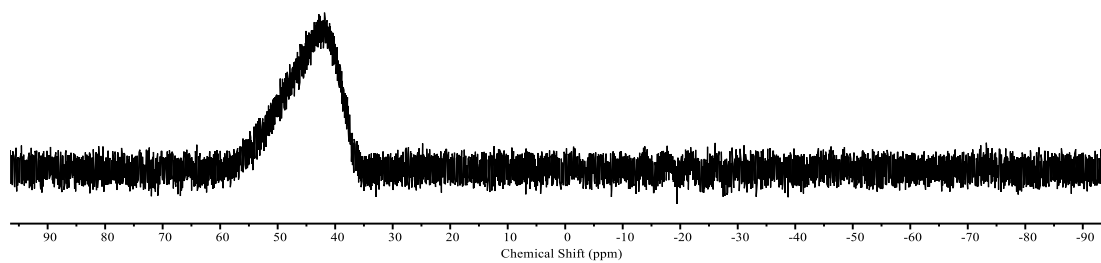
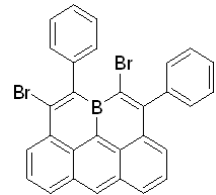


¹H NMR spectrum (400 MHz) of compound **BO-1** in CDCl₃ at 298 K.

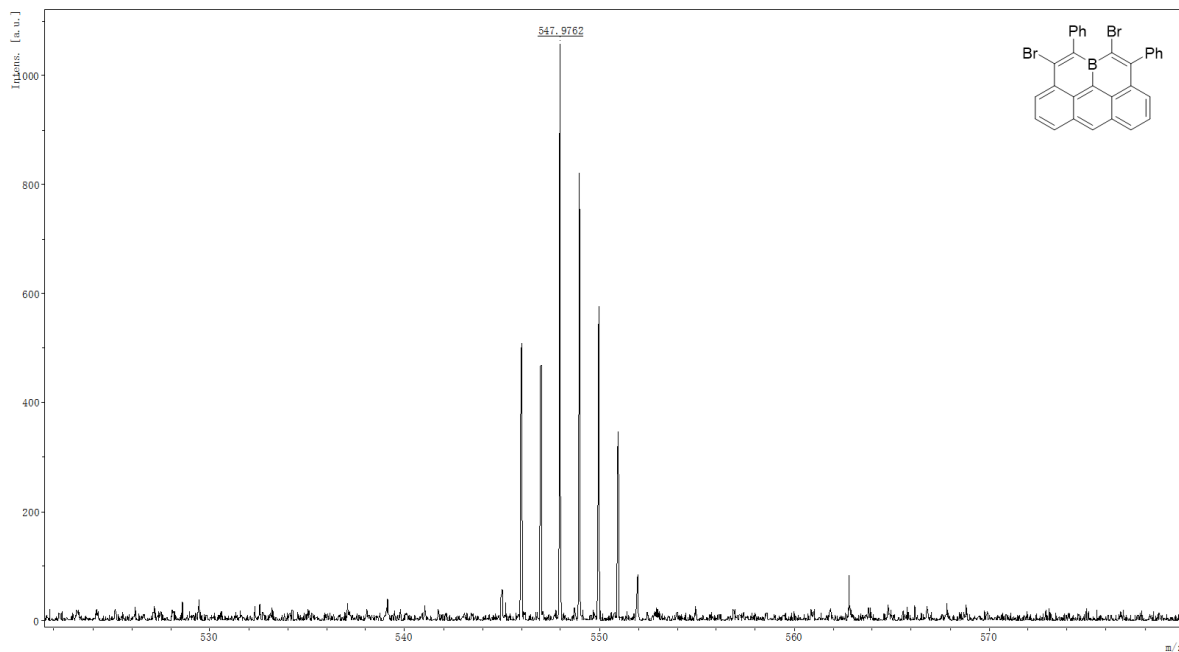


¹³C NMR spectrum (100 MHz) of compound **BO-1** in CDCl₃ at 298 K.

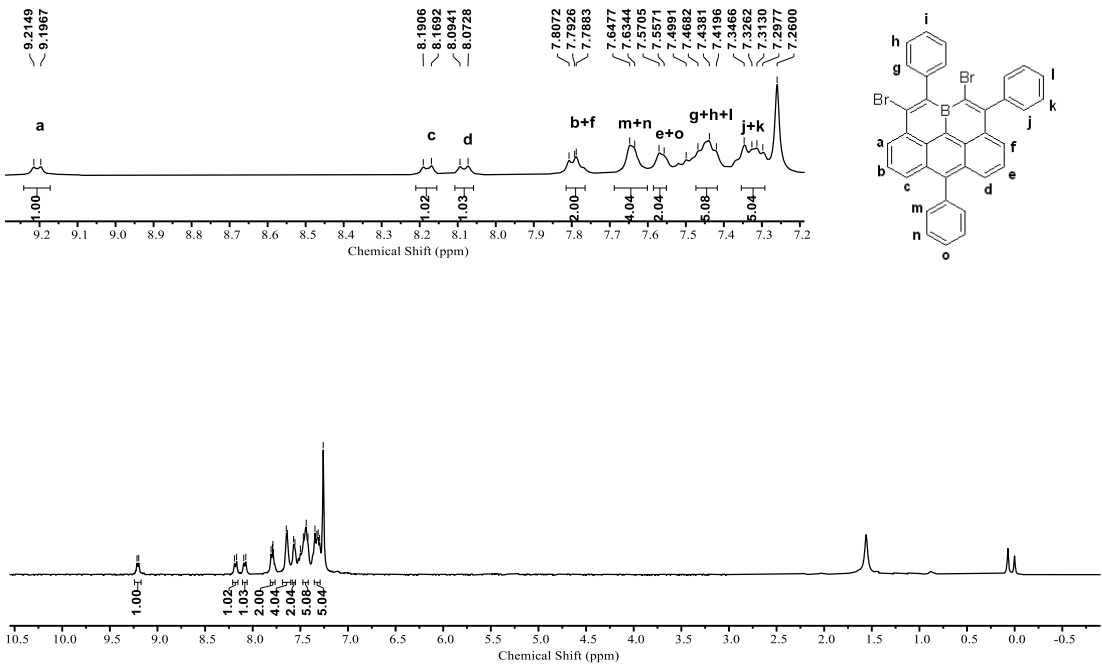
— 42.3089 —



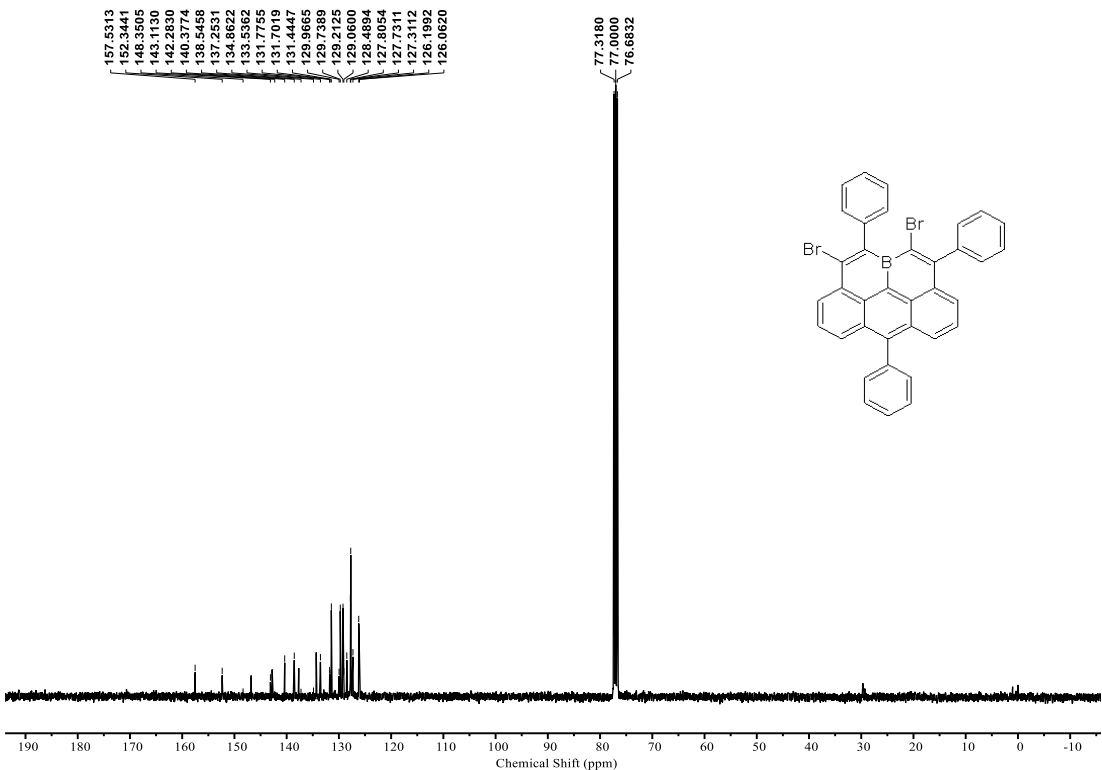
¹¹B NMR spectrum (128 MHz) of compound BO-1 in CDCl_3 at 298 K.



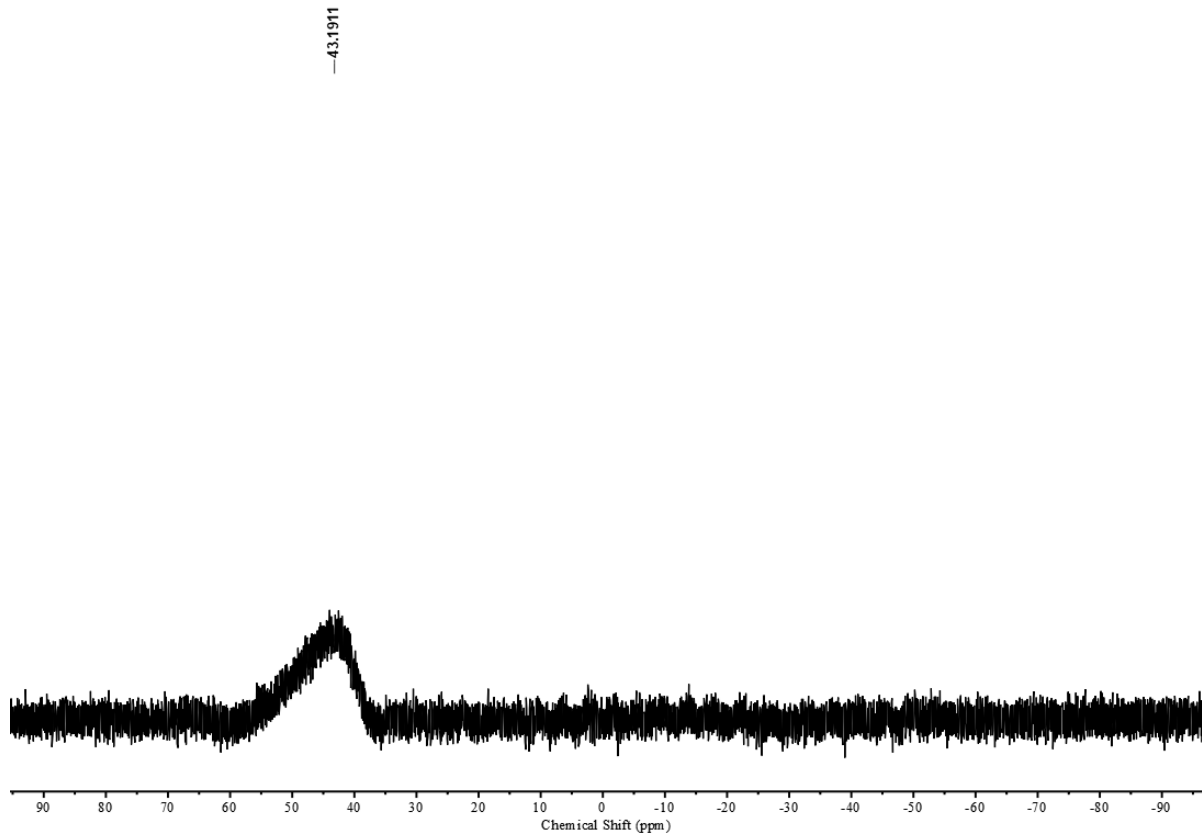
HR (MALDI-TOF) mass spectrum of compound BO-1.



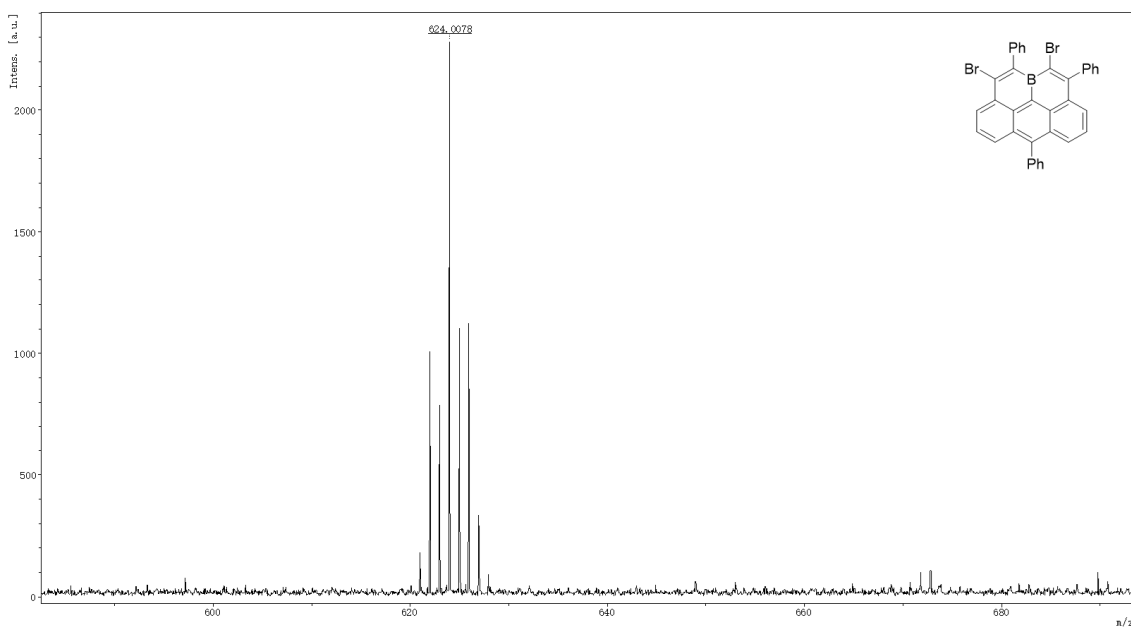
¹H NMR spectrum (400 MHz) of compound BO-2 in CDCl₃ at 298 K.



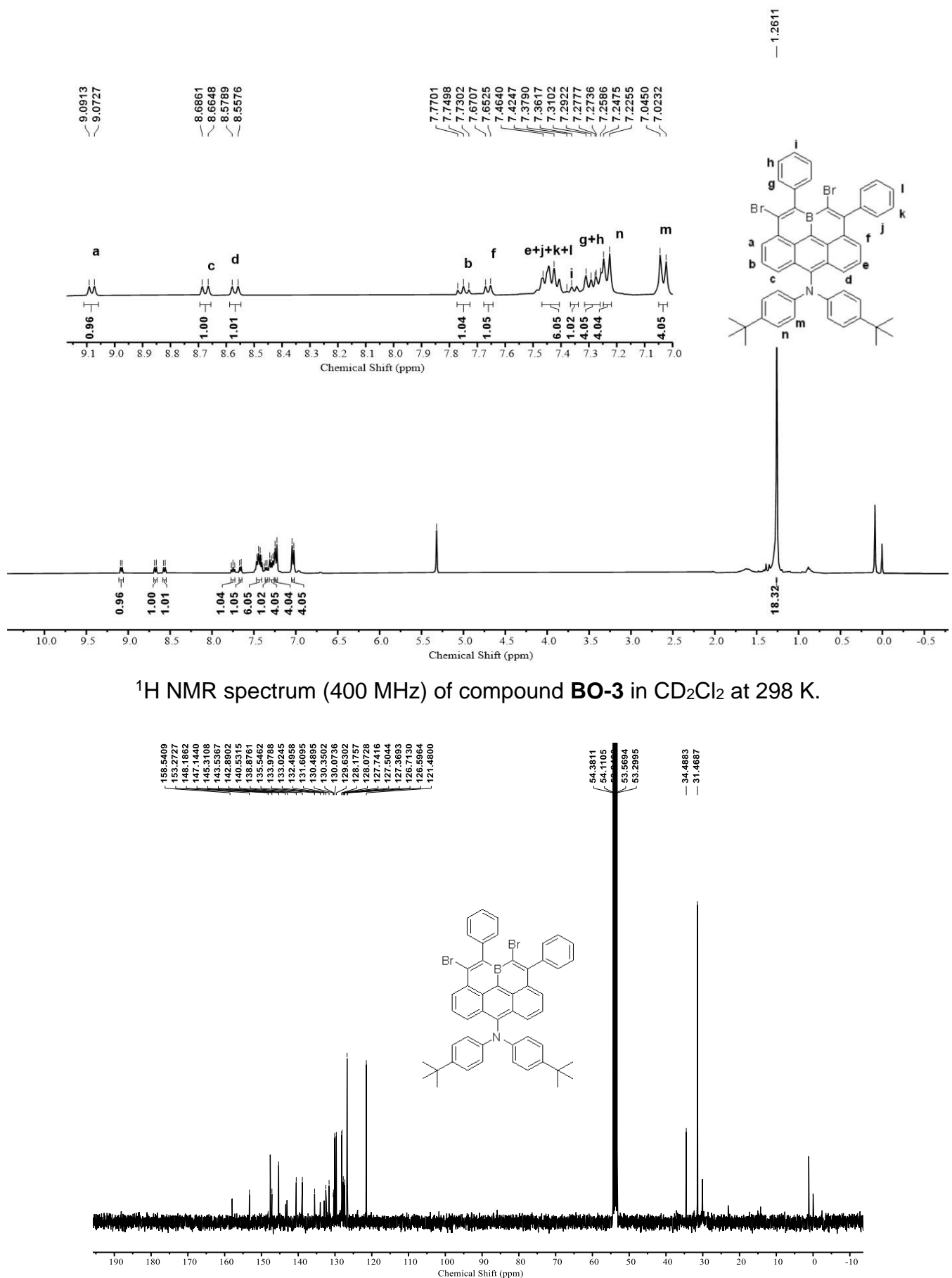
¹³C NMR spectrum (100 MHz) of compound **BO-2** in CDCl₃ at 298 K.



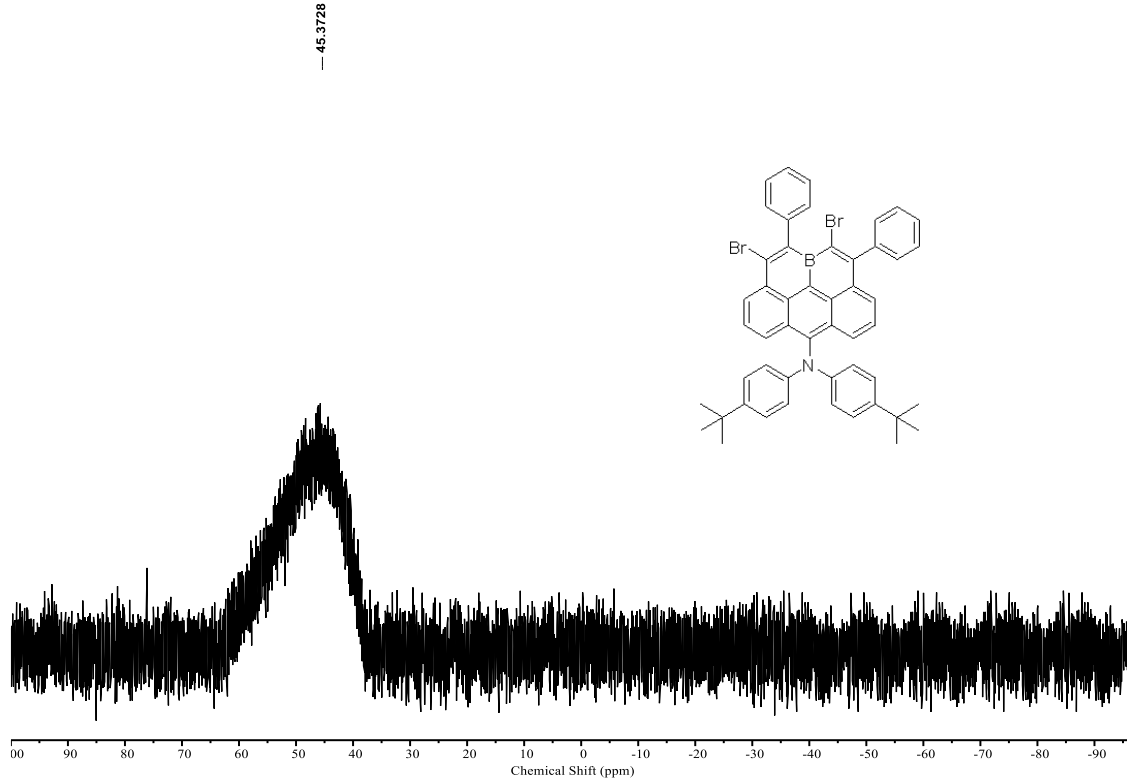
¹¹B NMR spectrum (128 MHz) of compound **BO-2** in CDCl₃ at 298 K.



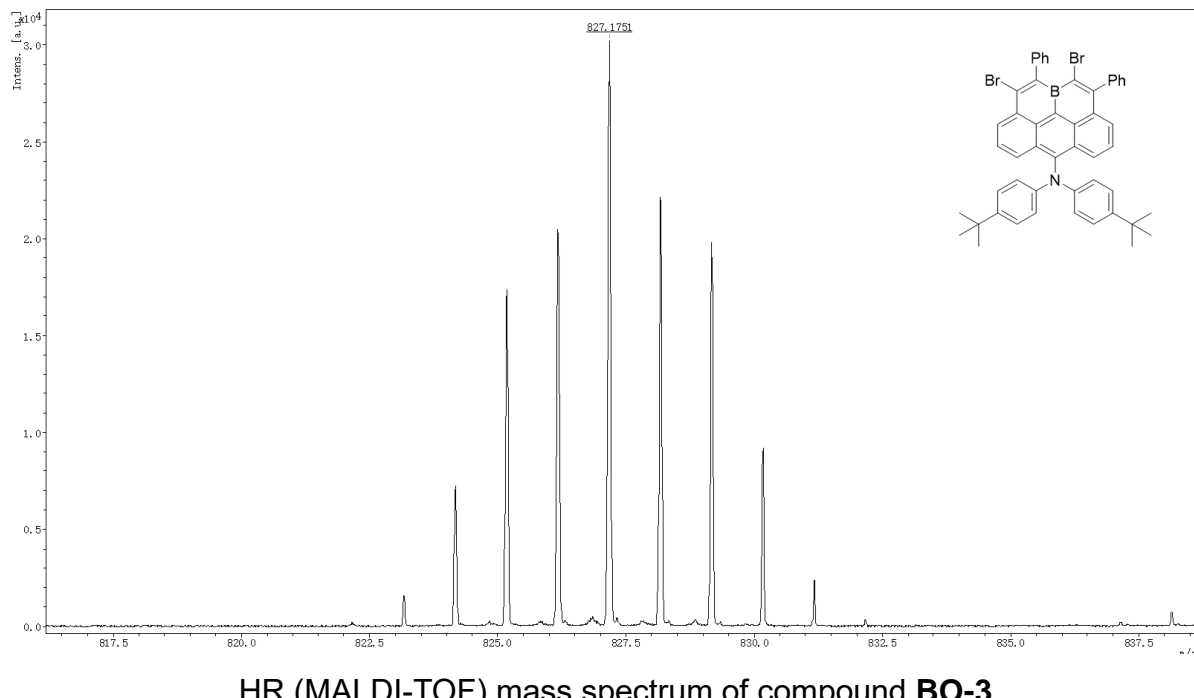
HR (MALDI-TOF) mass spectrum of compound **BO-2**.



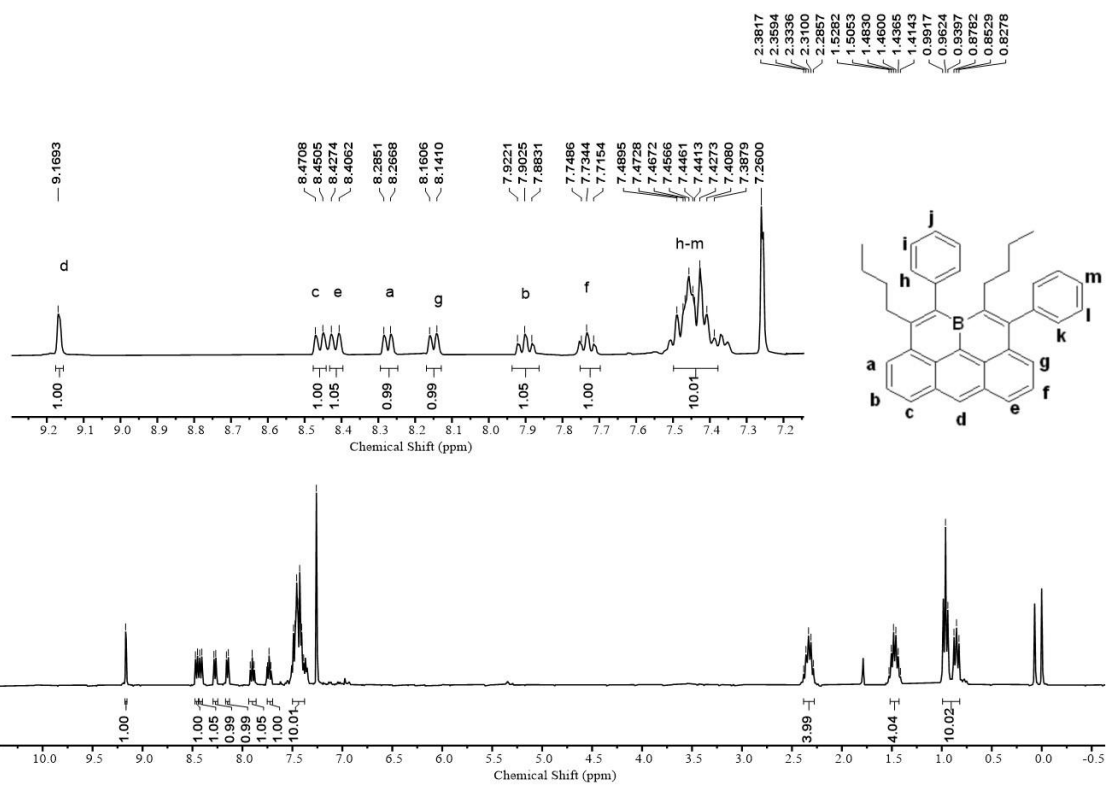
¹³C NMR spectrum (100 MHz) of compound **BO-3** in CD₂Cl₂ at 298 K.



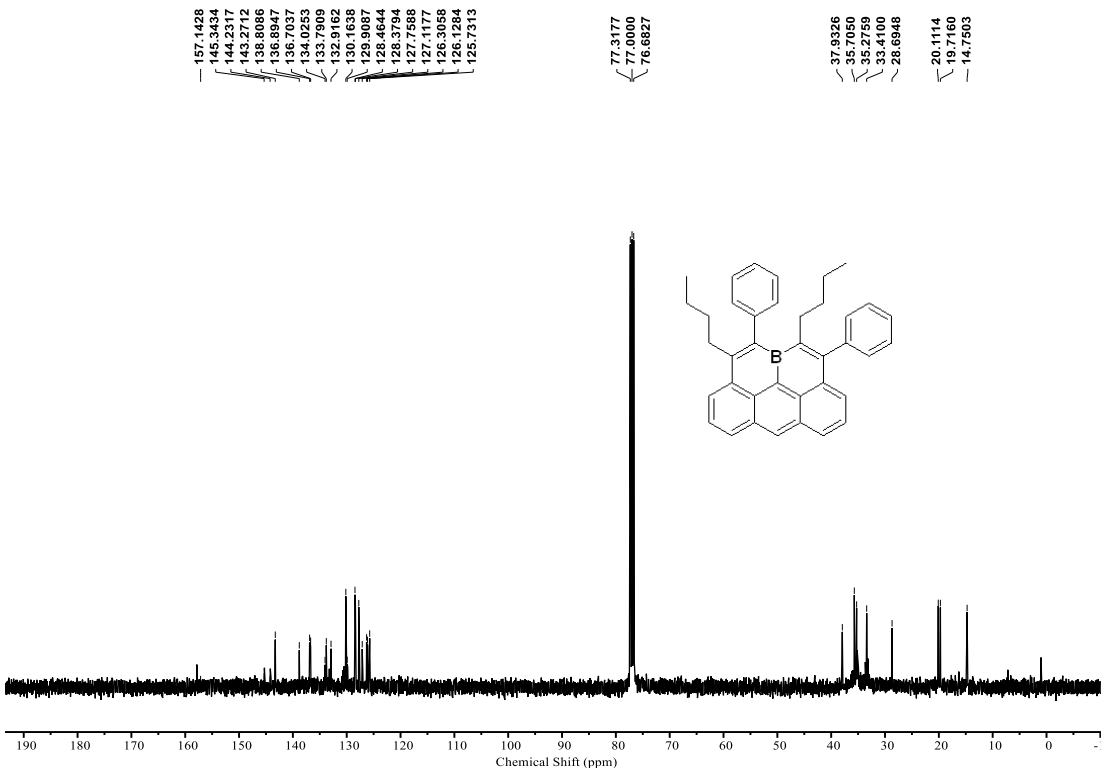
¹¹B NMR spectrum (128 MHz) of compound **BO-3** in CDCl₃ at 298 K.



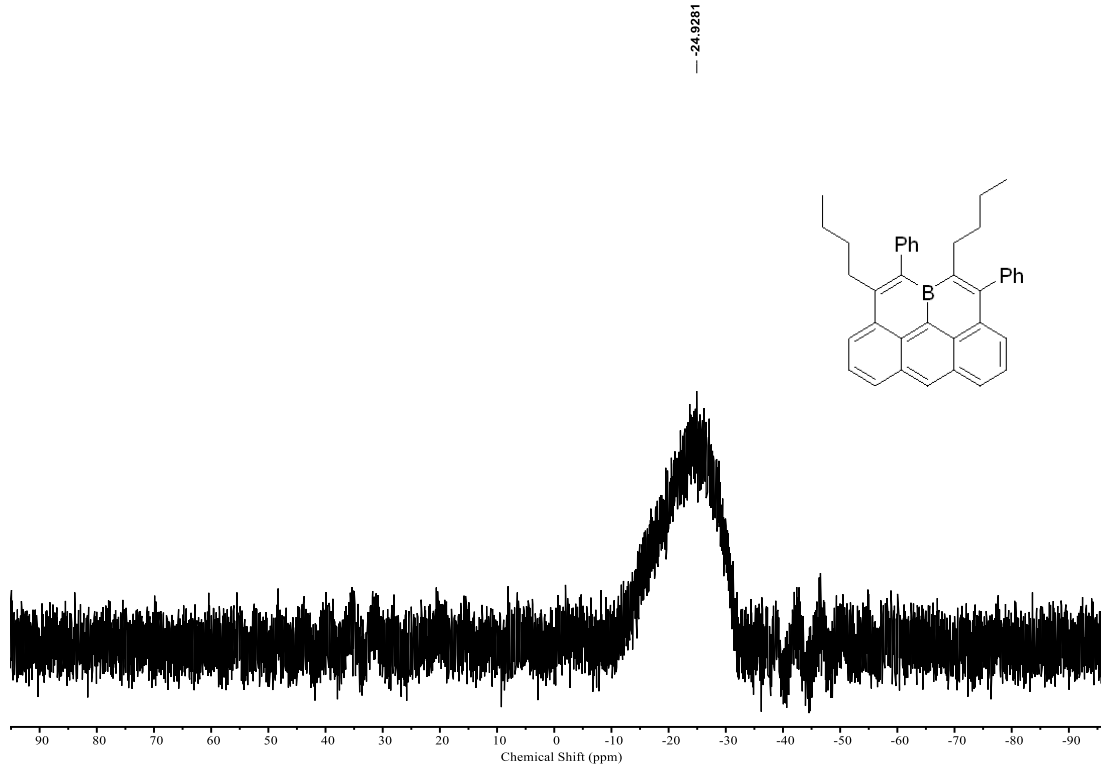
HR (MALDI-TOF) mass spectrum of compound **BO-3**.



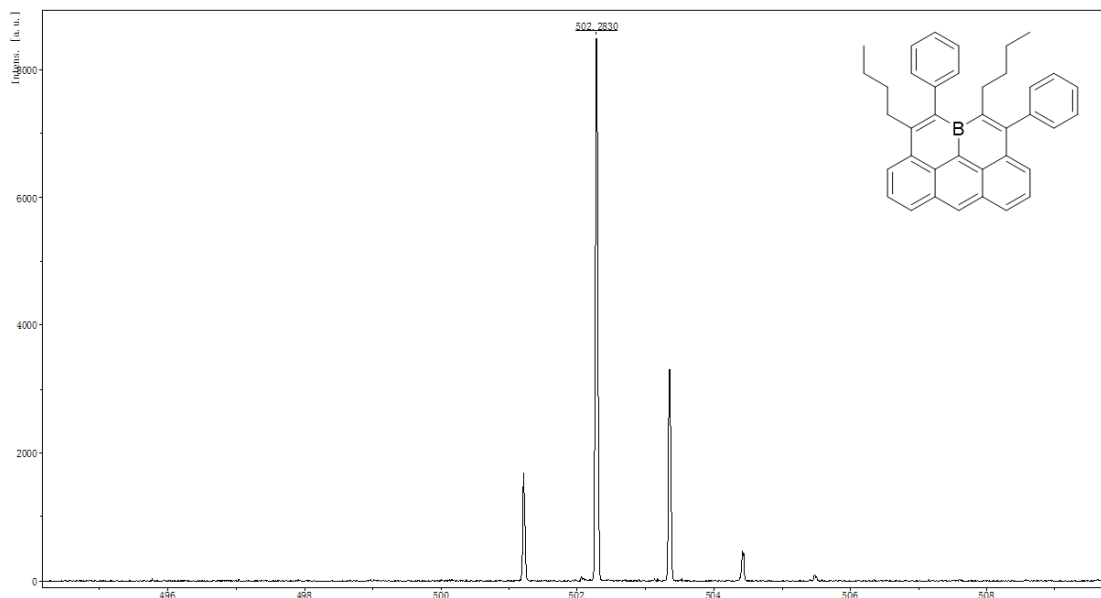
¹H NMR spectrum (400 MHz) of compound **BO-Bu** in CDCl₃ at 298 K.



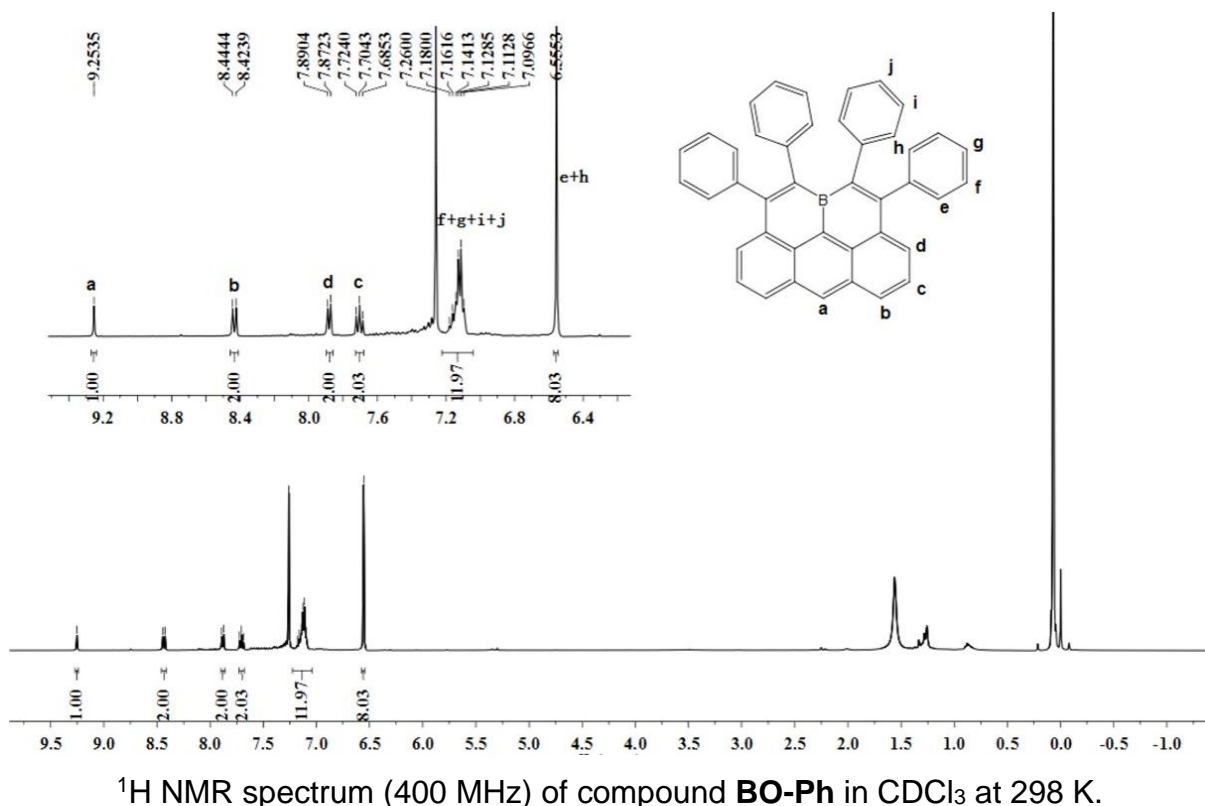
¹³C NMR spectrum (100 MHz) of compound **BO-Bu** in CDCl₃ at 298 K.



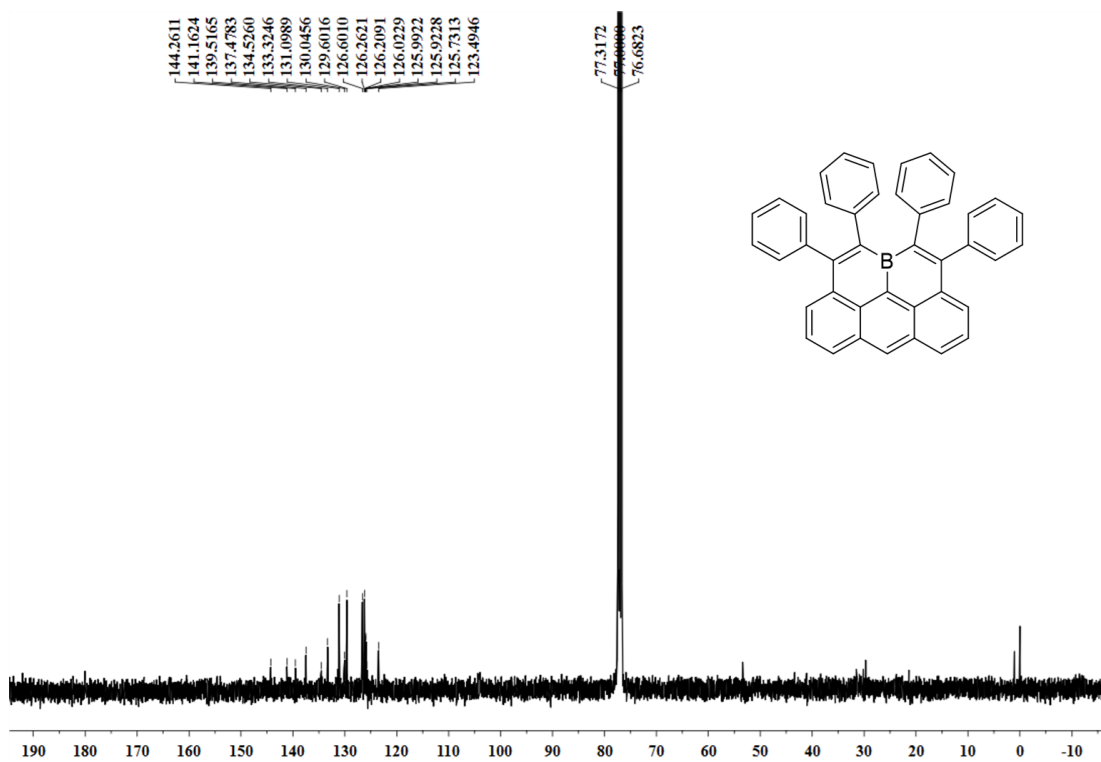
¹¹B NMR spectrum (128 MHz) of compound **BO-Bu** in CDCl₃ at 298 K.



HR (MALDI-TOF) mass spectrum of compound **BO-Bu**.

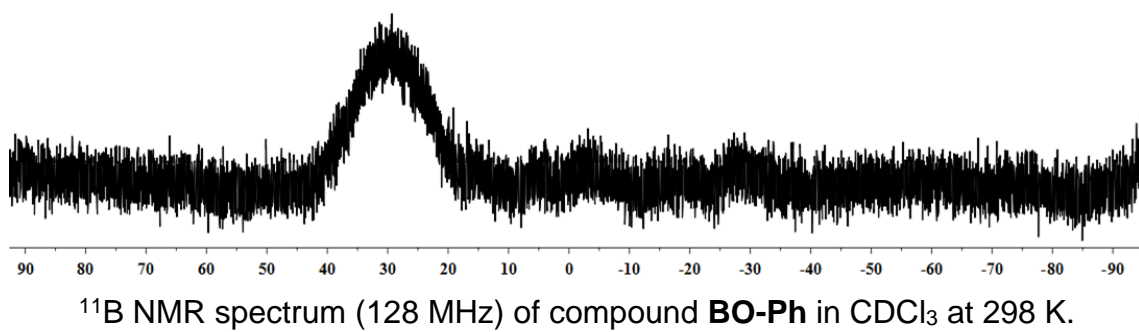
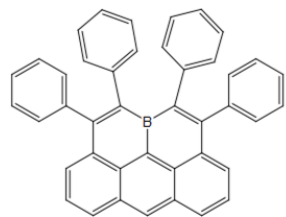


¹H NMR spectrum (400 MHz) of compound **BO-Ph** in CDCl₃ at 298 K.

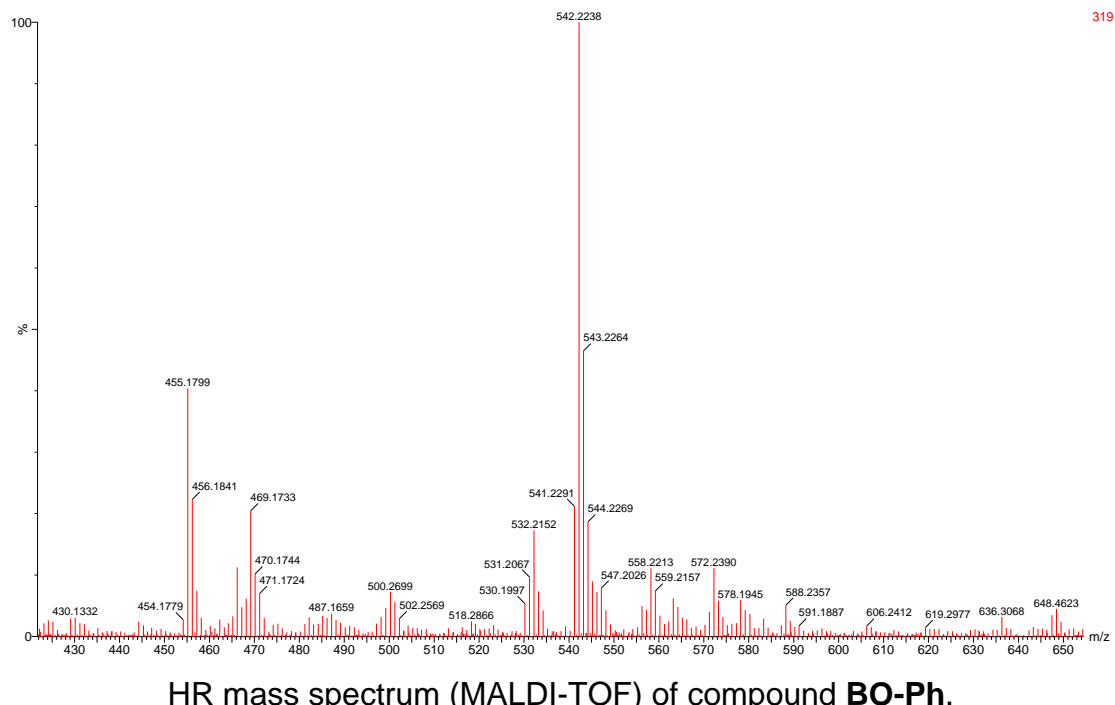


¹³C NMR spectrum (100 MHz) of compound **BO-Ph** in CDCl₃ at 298 K.

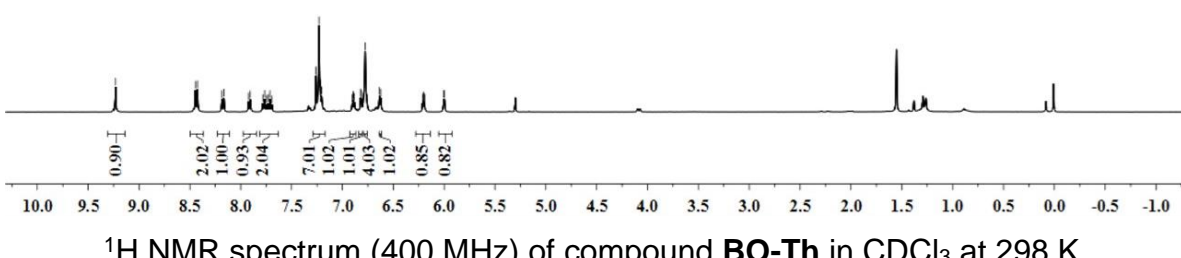
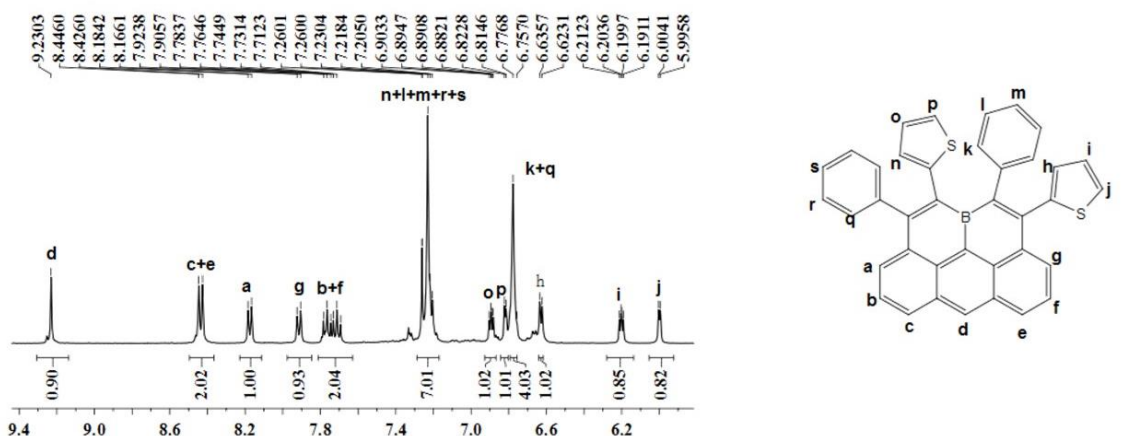
-29.5206



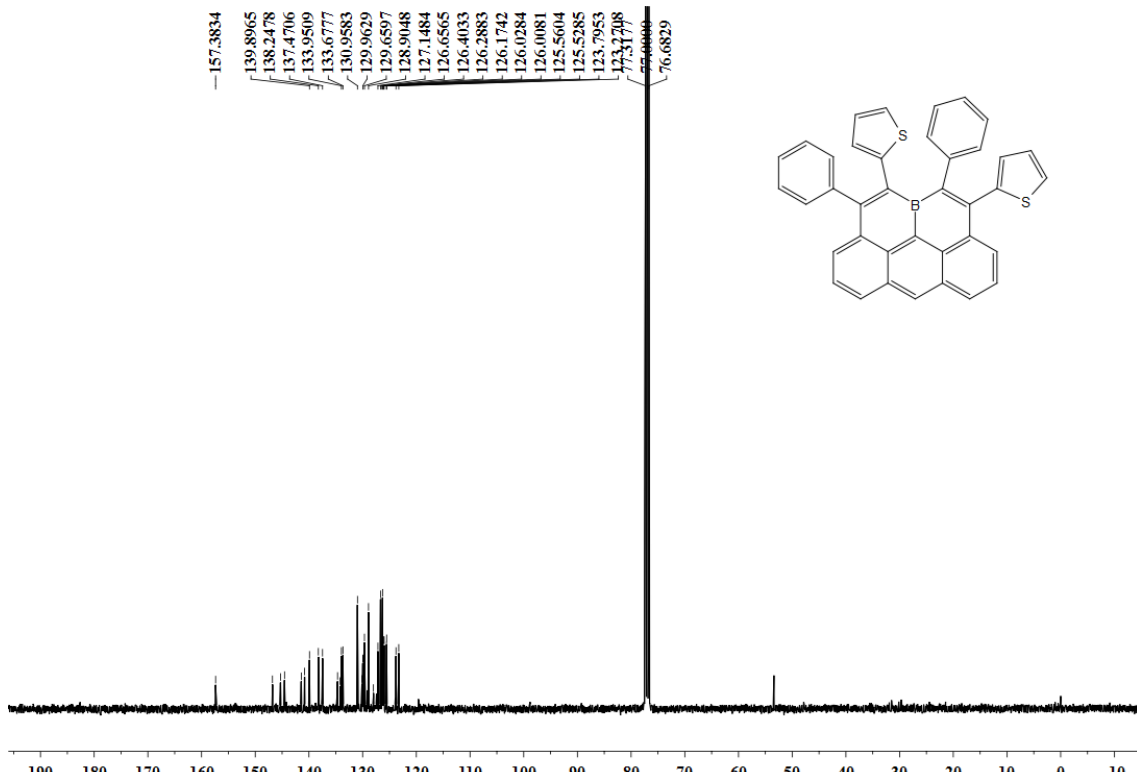
^{11}B NMR spectrum (128 MHz) of compound **BO-Ph** in CDCl_3 at 298 K.



HR mass spectrum (MALDI-TOF) of compound **BO-Ph**.

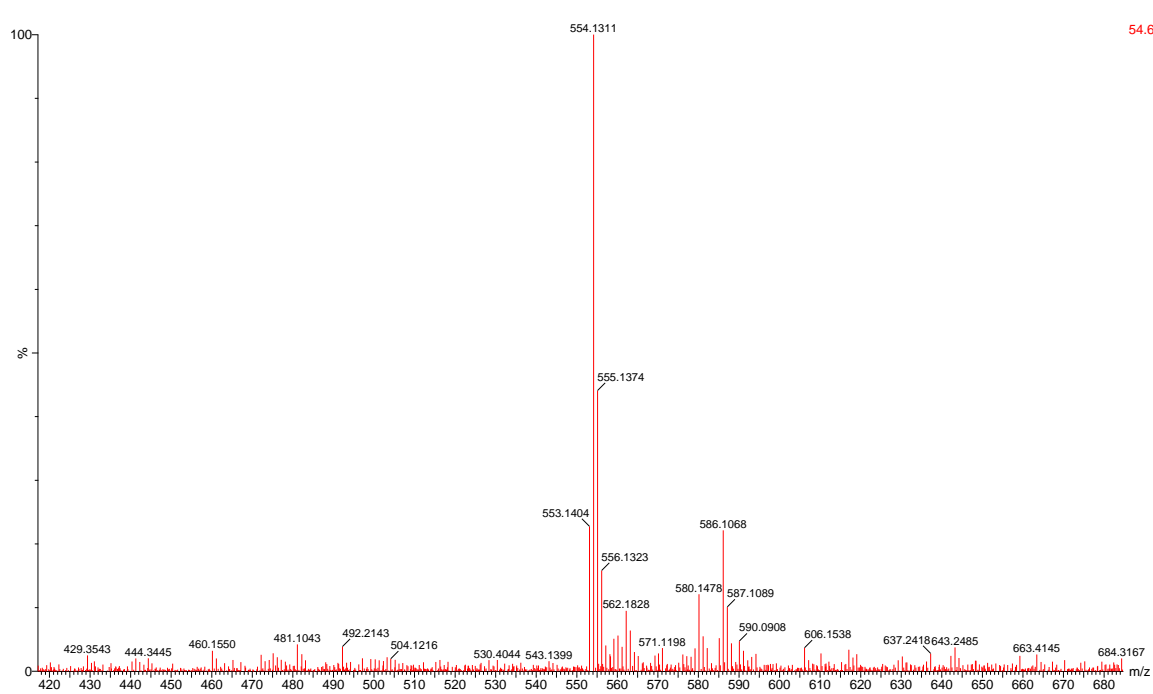
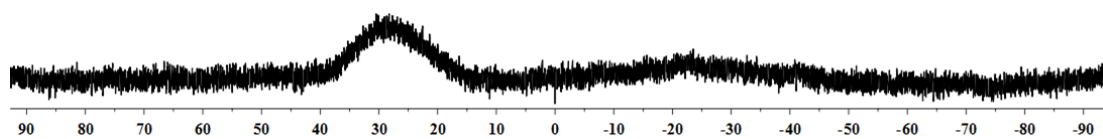
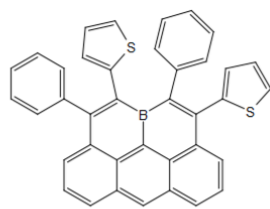


¹H NMR spectrum (400 MHz) of compound **BO-Th** in CDCl₃ at 298 K.



¹³C NMR spectrum (100 MHz) of compound **BO-Th** in CDCl₃ at 298 K.

-28.4223



Crystal data and structure refinement for **BO-1** (CCDC number: 1905586).

Identification code	BO-1
Empirical formula	C ₉₀ H ₅₁ B ₃ Br ₆
Formula weight	1644.20
Temperature/K	100.00(10)
Crystal system	triclinic
Space group	P1
a/Å	10.2031(2)
b/Å	11.8054(3)
c/Å	16.1220(4)
α/°	74.925(2)
β/°	89.781(2)
γ/°	89.984(2)
Volume/Å ³	1875.08(8)
Z	1
ρ _{calc} g/cm ³	1.456
μ/mm ⁻¹	4.216
F(000)	816.0
Crystal size/mm ³	0.2 × 0.08 × 0.05
Radiation	CuKα ($\lambda = 1.54184$)
2Θ range for data collection/°	7.756 to 130.17
Index ranges	-12 ≤ h ≤ 11, -13 ≤ k ≤ 13, -18 ≤ l ≤ 18
Reflections collected	25099
Independent reflections	11583 [R _{int} = 0.0492, R _{sigma} = 0.0770]
Data/restraints/parameters	11583/99/892
Goodness-of-fit on F ²	1.043
Final R indexes [I>=2σ (I)]	R ₁ = 0.0511, wR ₂ = 0.1240
Final R indexes [all data]	R ₁ = 0.0609, wR ₂ = 0.1289
Largest diff. peak/hole / e Å ⁻³	0.80/-0.76
Flack parameter	0.01(3)

Bond lengths for **BO-1**.

Atom	Atom	Length/Å	Atom	Atom	Length/Å
Br2	C8	1.922(11)	C11"	C12"	1.356(15)
Br1	C1	1.906(10)	C11"	C10"	1.405(15)
Br1'	C1'	1.941(10)	C12	C13	1.421(15)
Br2'	C8'	1.935(10)	C7'	C18'	1.371(16)
Br2"	C8"	1.906(11)	C2	C19	1.492(14)
Br1"	C1"	1.924(10)	C24	C23	1.405(16)
C5	C4	1.434(14)	C24	C19	1.390(17)
C5	C6	1.394(14)	C13	C14	1.396(14)
C5	B1	1.522(15)	C9"	C8"	1.368(16)
C6"	C15"	1.407(14)	C9"	C25"	1.470(15)
C6"	C7"	1.457(14)	C9"	B1"	1.554(16)
C6"	C5"	1.430(14)	C27'	C26'	1.391(15)
C8'	C9'	1.345(15)	C27'	C28'	1.371(18)
C8'	C7'	1.466(15)	C15'	C16'	1.440(15)
C15"	C14"	1.401(14)	C23	C22	1.385(19)
C15"	C16"	1.424(15)	C1'	C2'	1.356(16)
C6'	C5'	1.402(14)	C1'	B1'	1.529(16)
C6'	C7'	1.460(14)	C18	C17	1.394(17)
C6'	C15'	1.417(15)	C4"	C3"	1.457(14)
C5'	C4'	1.415(13)	C25	C26	1.370(17)
C5'	B1'	1.540(13)	C25	C30	1.407(17)
C4'	C13'	1.445(13)	C3'	C2'	1.473(14)
C4'	C3'	1.434(14)	C3"	C10"	1.376(15)
C11'	C10'	1.414(15)	C3"	C2"	1.460(15)
C11'	C12'	1.352(16)	C16	C17	1.375(17)
C7"	C18"	1.361(15)	C18'	C17'	1.418(16)
C7"	C8"	1.469(15)	C17'	C16'	1.362(17)
C4	C3	1.446(14)	C2'	C19'	1.492(15)
C4	C13	1.421(15)	C26'	C25'	1.390(17)
C11	C12	1.362(16)	C1"	C2"	1.361(16)

C11	C10	1.411(15)	C1"	B1"	1.535(16)
C17"	C18"	1.423(15)	C25'	C30'	1.387(17)
C17"	C16"	1.366(16)	C22	C21	1.381(19)
C5"	C4"	1.406(14)	C2"	C19"	1.513(14)
C5"	B1"	1.553(15)	C28'	C29'	1.39(2)
C13"	C12"	1.428(14)	C24'	C19'	1.400(18)
C13"	C4"	1.410(14)	C24'	C23'	1.343(19)
C13"	C14"	1.392(15)	C27"	C26"	1.375(18)
C14'	C13'	1.369(16)	C27"	C28"	1.40(2)
C14'	C15'	1.385(15)	C25"	C26"	1.372(19)
C3	C2	1.462(14)	C25"	C30"	1.392(18)
C3	C10	1.386(14)	C21"	C20"	1.388(18)
C9'	C25'	1.479(14)	C21"	C22"	1.37(2)
C9'	B1'	1.563(15)	C26	C27	1.371(17)
C6	C15	1.419(15)	C29	C28	1.40(2)
C6	C7	1.443(14)	C29	C30	1.373(19)
C9	C8	1.378(14)	C28	C27	1.39(2)
C9	C25	1.495(15)	C19"	C20"	1.41(2)
C9	B1	1.560(15)	C19"	C24"	1.39(2)
C20	C19	1.401(16)	C21'	C20'	1.370(18)
C20	C21	1.401(16)	C21'	C22'	1.40(2)
C1	C2	1.385(15)	C28"	C29"	1.35(2)
C1	B1	1.528(14)	C19'	C20'	1.395(17)
C10'	C3'	1.389(14)	C29'	C30'	1.379(17)
C12'	C13'	1.434(14)	C29"	C30"	1.414(17)
C15	C16	1.430(15)	C22"	C23"	1.35(2)
C15	C14	1.406(15)	C23'	C22'	1.37(2)
C8	C7	1.460(15)	C23"	C24"	1.425(17)
C7	C18	1.391(15)			

Bond angles for BO-1.

Atom	Atom	Atom	Angle/	Atom	Atom	Atom	Angle/
C4	C5	B1	119.2(9)	C2'	C1'	B1'	124.0(9)

C6	C5	C4	119.3(9)	B1'	C1'	Br1'	120.7(8)
C6	C5	B1	121.5(9)	C7	C18	C17	122.6(10)
C15"	C6"	C7"	118.6(9)	C3	C10	C11	123.1(10)
C15"	C6"	C5"	121.1(9)	C5"	C4"	C13"	121.1(10)
C5"	C6"	C7"	120.3(9)	C5"	C4"	C3"	120.2(9)
C9'	C8'	Br2'	118.2(8)	C13"	C4"	C3"	118.6(9)
C9'	C8'	C7'	127.5(9)	C13"	C14"	C15"	121.9(9)
C7'	C8'	Br2'	114.1(7)	C26	C25	C9	122.0(11)
C6"	C15"	C16"	120.6(9)	C26	C25	C30	118.7(11)
C14"	C15"	C6"	118.6(9)	C30	C25	C9	119.0(11)
C14"	C15"	C16"	120.8(9)	C4'	C3'	C2'	120.7(9)
C5'	C6'	C7'	120.7(9)	C10'	C3'	C4'	118.7(9)
C5'	C6'	C15'	120.6(9)	C10'	C3'	C2'	120.6(10)
C15'	C6'	C7'	118.6(10)	C4"	C3"	C2"	120.4(9)
C6'	C5'	C4'	119.1(9)	C10"	C3"	C4"	117.8(10)
C6'	C5'	B1'	120.6(9)	C10"	C3"	C2"	121.8(10)
C4'	C5'	B1'	120.0(9)	C3"	C10"	C11"	122.8(10)
C5'	C4'	C13'	119.4(9)	C17	C16	C15	118.3(10)
C5'	C4'	C3'	121.5(9)	C13	C14	C15	121.5(10)
C3'	C4'	C13'	119.1(9)	C20	C19	C2	120.0(11)
C12'	C11'	C10'	120.3(10)	C24	C19	C20	119.9(10)
C6"	C7"	C8"	119.1(9)	C24	C19	C2	120.1(10)
C18"	C7"	C6"	118.2(10)	C7"	C18"	C17"	123.3(10)
C18"	C7"	C8"	122.6(10)	C7'	C18'	C17'	121.9(10)
C5	C4	C3	120.2(9)	C17"	C16"	C15"	120.4(10)
C13	C4	C5	120.0(9)	C7"	C8"	Br2"	115.8(8)
C13	C4	C3	119.8(9)	C9"	C8"	Br2"	118.1(8)
C12	C11	C10	119.5(9)	C9"	C8"	C7"	126.1(10)
C16"	C17"	C18"	118.9(10)	C16'	C17'	C18'	120.5(10)
C6"	C5"	B1"	119.9(9)	C1'	C2'	C3'	119.5(10)
C4"	C5"	C6"	118.1(9)	C1'	C2'	C19'	123.6(10)
C4"	C5"	B1"	122.0(9)	C3'	C2'	C19'	116.9(9)

C4"	C13"	C12"	120.5(10)	C25'	C26'	C27'	122.6(11)
C14"	C13"	C12"	120.3(9)	C16	C17	C18	121.0(10)
C14"	C13"	C4"	119.2(9)	C2"	C1"	Br1"	115.4(8)
C13'	C14'	C15'	122.1(9)	C2"	C1"	B1"	123.7(9)
C4	C3	C2	121.6(9)	B1"	C1"	Br1"	120.9(8)
C10	C3	C4	117.2(9)	C17'	C16'	C15'	120.0(10)
C10	C3	C2	121.1(10)	C26'	C25'	C9'	119.6(10)
C8'	C9'	C25'	121.4(10)	C30'	C25'	C9'	123.4(11)
C8'	C9'	B1'	116.1(9)	C30'	C25'	C26'	116.9(10)
C25'	C9'	B1'	122.5(9)	C21	C22	C23	120.5(10)
C5	C6	C15	120.9(10)	C3"	C2"	C19"	115.0(9)
C5	C6	C7	121.0(9)	C1"	C2"	C3"	121.0(9)
C15	C6	C7	118.0(9)	C1"	C2"	C19"	123.9(10)
C8	C9	C25	120.1(10)	C27'	C28'	C29'	119.1(11)
C8	C9	B1	116.5(10)	C22	C21	C20	120.0(11)
C25	C9	B1	123.5(9)	C23'	C24'	C19'	121.4(14)
C21	C20	C19	119.7(12)	C26"	C27"	C28"	118.7(13)
C2	C1	Br1	115.6(7)	C26"	C25"	C9"	121.4(11)
C2	C1	B1	120.4(9)	C26"	C25"	C30"	118.0(11)
B1	C1	Br1	123.9(8)	C30"	C25"	C9"	120.5(11)
C3'	C10'	C11'	122.0(10)	C22"	C21"	C20"	121.8(14)
C11'	C12'	C13'	121.1(10)	C25	C26	C27	121.7(13)
C6	C15	C16	121.8(10)	C30	C29	C28	119.2(13)
C14	C15	C6	119.1(10)	C27	C28	C29	120.3(11)
C14	C15	C16	119.1(10)	C25"	C26"	C27"	123.1(15)
C9	C8	Br2	117.9(8)	C20"	C19"	C2"	120.4(12)
C9	C8	C7	125.6(10)	C24"	C19"	C2"	118.8(12)
C7	C8	Br2	116.5(7)	C24"	C19"	C20"	120.8(11)
C14'	C13'	C4'	119.3(9)	C5'	B1'	C9'	116.7(9)
C14'	C13'	C12'	122.2(9)	C1'	B1'	C5'	113.9(9)
C12'	C13'	C4'	118.6(10)	C1'	B1'	C9'	129.4(9)
C6	C7	C8	118.6(9)	C21"	C20"	C19"	117.9(14)

C18	C7	C6	118.3(10)	C20'	C21'	C22'	120.3(14)
C18	C7	C8	123.1(10)	C29	C30	C25	120.7(13)
C12"	C11"	C10"	120.2(10)	C29"	C28"	C27"	119.5(11)
C11	C12	C13	120.9(10)	C24'	C19'	C2'	120.6(11)
C6'	C7'	C8'	117.6(9)	C20'	C19'	C2'	121.8(11)
C18'	C7'	C8'	123.4(10)	C20'	C19'	C24'	117.6(11)
C18'	C7'	C6'	118.9(10)	C30'	C29'	C28'	121.2(12)
C3	C2	C19	118.2(9)	C5	B1	C9	116.7(9)
C1	C2	C3	120.7(9)	C5	B1	C1	117.3(10)
C1	C2	C19	121.1(9)	C1	B1	C9	125.9(10)
C19	C24	C23	119.8(11)	C28"	C29"	C30"	121.2(14)
C4	C13	C12	119.5(9)	C5"	B1"	C9"	117.6(10)
C14	C13	C4	119.1(9)	C1"	B1"	C5"	112.6(9)
C14	C13	C12	121.4(10)	C1"	B1"	C9"	129.7(10)
C11"	C12"	C13"	119.9(9)	C21'	C20'	C19'	120.8(13)
C8"	C9"	C25"	120.2(10)	C26	C27	C28	119.3(13)
C8"	C9"	B1"	116.8(10)	C23"	C22"	C21"	120.8(12)
C25"	C9"	B1"	123.0(10)	C29'	C30'	C25'	121.0(12)
C28'	C27'	C26'	119.3(12)	C24'	C23'	C22'	121.6(16)
C6'	C15'	C16'	119.9(10)	C25"	C30"	C29"	119.4(13)
C14'	C15'	C6'	119.4(10)	C23'	C22'	C21'	118.3(13)
C14'	C15'	C16'	120.7(10)	C22"	C23"	C24"	120.2(14)
C22	C23	C24	120.0(12)	C19"	C24"	C23"	118.5(14)
C2'	C1'	Br1'	115.3(8)				

Crystal data and structure refinement for **BO-2** (CCDC number: 2235180).

Identification code	BO-2
Empirical formula	C ₃₇ H ₂₂ BBr ₂ Cl ₃
Formula weight	743.52
Temperature/K	99.98(11)
Crystal system	triclinic

Space group	P1
a/Å	9.6748(3)
b/Å	10.1293(4)
c/Å	17.5132(6)
$\alpha/^\circ$	97.089(3)
$\beta/^\circ$	94.219(3)
$\gamma/^\circ$	117.910(3)
Volume/Å ³	1488.07(10)
Z	2
$\rho_{\text{calc}} \text{g/cm}^3$	1.659
μ/mm^{-1}	6.142
F(000)	740.0
Crystal size/mm ³	0.3 × 0.1 × 0.05
Radiation	CuKα ($\lambda = 1.54184$)
2Θ range for data collection/°	5.142 to 133.176
Index ranges	-11 ≤ h ≤ 10, -12 ≤ k ≤ 11, -20 ≤ l ≤ 20
Reflections collected	9009
Independent reflections	5221 [$R_{\text{int}} = 0.0517$, $R_{\text{sigma}} = 0.0651$]
Data/restraints/parameters	5221/0/388
Goodness-of-fit on F ²	1.070
Final R indexes [$ I >= 2\sigma(I)$]	$R_1 = 0.0621$, $wR_2 = 0.1779$
Final R indexes [all data]	$R_1 = 0.0704$, $wR_2 = 0.1916$
Largest diff. peak/hole / e Å ⁻³	1.74/-1.29

Bond lengths for BO-2.

Atom	Atom	Length/Å	Atom	Atom	Length/Å
Br1	C8	1.926(5)	C13	C14	1.395(7)
Br2	C26	1.921(4)	C22	C21	1.422(7)
Cl2	C37	1.766(6)	C22	C23	1.362(7)

Cl1	C37	1.751(6)	C25	C26	1.456(7)
Cl3	C37	1.765(6)	C25	C24	1.380(7)
C9	C29	1.439(7)	C7	C2	1.493(7)
C9	C7	1.470(6)	C16	C17	1.404(7)
C9	C10	1.390(7)	C16	C15	1.403(7)
C30	C28	1.402(7)	C2	C1	1.386(7)
C30	C25	1.446(6)	C2	C3	1.403(7)
C30	C21	1.429(6)	C36	C35	1.399(7)
C31	C27	1.483(6)	C11	C10	1.423(7)
C31	C36	1.402(7)	C35	C34	1.385(8)
C31	C32	1.385(7)	C6	C1	1.389(7)
C28	C29	1.414(7)	C6	C5	1.391(8)
C28	B1	1.538(7)	C17	C18	1.390(8)
C33	C32	1.403(7)	C24	C23	1.415(7)
C33	C34	1.378(8)	C21	C14	1.417(7)
C12	C13	1.440(6)	C15	C14	1.495(6)
C12	C11	1.336(7)	C15	C20	1.401(7)
C8	C7	1.367(7)	C4	C3	1.397(7)
C8	B1	1.537(7)	C4	C5	1.376(8)
C29	C13	1.425(6)	C19	C18	1.392(8)
C27	C26	1.353(7)	C19	C20	1.396(7)
C27	B1	1.561(6)			

Bond angles for BO-2.

Atom	Atom	Atom	Angle/	Atom	Atom	Atom	Angle/
C29	C9	C7	121.8(4)	C3	C2	C7	121.2(4)
C10	C9	C29	118.5(4)	C35	C36	C31	120.4(5)
C10	C9	C7	119.7(4)	C31	C32	C33	120.6(5)
C28	C30	C25	120.3(4)	C12	C11	C10	120.4(4)
C28	C30	C21	121.1(4)	C34	C35	C36	119.9(5)
C21	C30	C25	118.5(4)	C1	C6	C5	119.6(5)
C36	C31	C27	120.8(4)	C18	C17	C16	119.7(5)
C32	C31	C27	120.3(4)	C27	C26	Br2	118.8(3)

C32	C31	C36	118.8(4)	C27	C26	C25	126.7(4)
C30	C28	C29	118.6(4)	C25	C26	Br2	114.5(3)
C30	C28	B1	120.7(4)	C25	C24	C23	122.4(4)
C29	C28	B1	120.6(4)	C22	C21	C30	119.8(4)
C34	C33	C32	120.2(5)	C14	C21	C30	119.2(4)
C11	C12	C13	121.5(4)	C14	C21	C22	121.0(4)
C7	C8	Br1	116.0(4)	C16	C15	C14	119.4(5)
C7	C8	B1	122.1(4)	C20	C15	C16	119.0(5)
B1	C8	Br1	121.8(3)	C20	C15	C14	121.6(4)
C28	C29	C9	119.7(4)	C22	C23	C24	119.7(5)
C28	C29	C13	120.7(4)	C2	C1	C6	120.9(4)
C13	C29	C9	119.6(4)	C9	C10	C11	121.2(4)
C31	C27	B1	123.7(4)	C5	C4	C3	120.8(5)
C26	C27	C31	120.1(4)	C18	C19	C20	120.4(5)
C26	C27	B1	116.1(4)	C33	C34	C35	120.1(5)
C29	C13	C12	118.2(4)	C4	C3	C2	119.3(5)
C14	C13	C12	121.7(4)	C13	C14	C21	120.0(4)
C14	C13	C29	120.0(4)	C13	C14	C15	120.8(4)
C23	C22	C21	120.8(4)	C21	C14	C15	119.1(4)
C30	C25	C26	118.9(4)	C4	C5	C6	120.0(5)
C24	C25	C30	118.7(4)	C17	C18	C19	120.1(5)
C24	C25	C26	122.4(4)	C19	C20	C15	120.2(5)
C9	C7	C2	116.2(4)	Cl1	C37	Cl2	111.9(3)
C8	C7	C9	119.5(4)	Cl1	C37	Cl3	109.7(3)
C8	C7	C2	124.3(4)	Cl3	C37	Cl2	109.8(3)
C15	C16	C17	120.5(5)	C28	B1	C27	117.0(4)
C1	C2	C7	119.4(4)	C8	B1	C28	114.8(4)
C1	C2	C3	119.4(5)	C8	B1	C27	128.1(4)

9. References

[S1] Gaussian 09, Revision D.01, M. J. Frisch, G. W. Trucks, H. B. Schlegel, G. E. Scuseria, M. A. Robb, J. R. Cheeseman, G. Scalmani, V. Barone, B. Mennucci, G. A. Petersson, H. Nakatsuji, M. Caricato, X. Li, H. P. Hratchian, A. F. Izmaylov, J. Bloino, G. Zheng, J. L. Sonnenberg, M. Hada, M. Ehara, K. Toyota, R. Fukuda, J. Hasegawa, M. Ishida, T. Nakajima, Y. Honda, O. Kitao, H. Nakai, T. Vreven, J. A. Montgomery, Jr., J. E. Peralta, F. Ogliaro, M. Bearpark, J. J. Heyd, E. Brothers, K. N. Kudin, V. N. Staroverov, T. Keith, R. Kobayashi, J. Normand, K. Raghavachari, A. Rendell, J. C. Burant, S. S. Iyengar, J. Tomasi, M. Cossi, N. Rega, J. M. Millam, M. Klene, J. E. Knox, J. B. Cross, V. Bakken, C. Adamo, J. Jaramillo, R. Gomperts, R. E. Stratmann, O. Yazyev, A. J. Austin, R. Cammi, C. Pomelli, J. W. Ochterski, R. L. Martin, K. Morokuma, V. G. Zakrzewski, G. A. Voth, P. Salvador, J. J. Dannenberg, S. Dapprich, A. D. Daniels, O. Farkas, J. B. Foresman, J. V. Ortiz, J. Cioslowski, and D. J. Fox, Gaussian, Inc., Wallingford CT, **2010**.